


Review

Recent Advances in Metal Catalyst Design for CO₂ Hydroboration to C1 Derivatives

 Sylwia Kostera, Maurizio Peruzzini and Luca Gonsalvi * 

Consiglio Nazionale delle Ricerche (CNR), Istituto di Chimica dei Composti Organometallici (ICCOM), Via Madonna del Piano 10, 50019 Sesto Fiorentino, Firenze, Italy; sylwia.kostera@iccom.cnr.it (S.K.); maurizio.peruzzini@iccom.cnr.it (M.P.)

* Correspondence: l.gonsalvi@iccom.cnr.it; Tel.: +39-055-5225251

Abstract: The use of CO₂ as a C1 building block for chemical synthesis is receiving growing attention, due to the potential of this simple molecule as an abundant and cheap renewable feedstock. Among the possible reductants used in the literature to bring about CO₂ reduction to C1 derivatives, hydroboranes have found various applications, in the presence of suitable homogeneous catalysts. The current minireview article summarizes the main results obtained since 2016 in the synthetic design of main group, first and second row transition metals for use as catalysts for CO₂ hydroboration.

Keywords: carbon dioxide conversion; hydroboration; homogeneous catalysis; metal complexes

1. Introduction

In recent years, the accumulation of greenhouse gases in the atmosphere has steadily increased due to human activity [1]. The combustion of fossil fuels for the production of energy is the largest source of greenhouse gas emissions [2]. CO₂ is a by-product of fuel combustion, representing the most abundant greenhouse gas (81.3%) of the global anthropogenic emissions (Figure 1). A significant increase of CO₂ in the atmosphere is expected in view of growing demand for energy [3]. These reasons, combined with the need for sustainable, fossil-free routes to chemicals and fuels, fostered a new impetus in the use of CO₂ as a C1 building block for chemical synthesis [1].

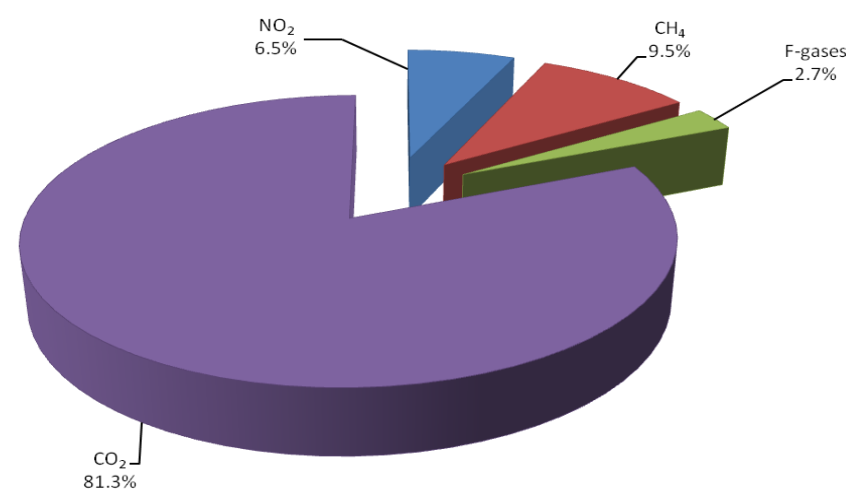


Figure 1. Global greenhouse gas emission per type of gas in 2018 [1].

Carbon dioxide can be used to make added value products, by reactions such as copolymerization [4], hydrogenation [5,6], biochemical approaches [7], and electrochemical reduction [7,8]. Recently, there has been an increase in interest in the homogeneous



Citation: Kostera, S.; Peruzzini, M.; Gonsalvi, L. Recent Advances in Metal Catalyst Design for CO₂ Hydroboration to C1 Derivatives. *Catalysts* **2021**, *11*, 58. <https://doi.org/10.3390/catal11010058>

Received: 2 December 2020

Accepted: 30 December 2020

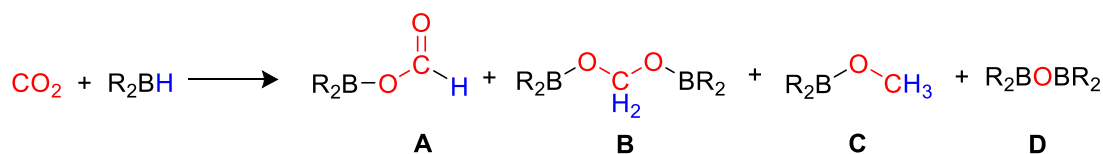
Published: 2 January 2021

Publisher's Note: MDPI stays neutral with regard to jurisdictional claims in published maps and institutional affiliations.



Copyright: © 2021 by the authors. Licensee MDPI, Basel, Switzerland. This article is an open access article distributed under the terms and conditions of the Creative Commons Attribution (CC BY) license (<https://creativecommons.org/licenses/by/4.0/>).

reduction of CO₂ using hydrogen [9–11], hydrosilanes [12–15] and hydroborates [16,17]. Reductive approaches allow to obtain simple C1 molecules such as formic acid (HCO₂H), formaldehyde (HCHO), methanol (CH₃OH), dimethyl ether (CH₃OCH₃), methane (CH₄) or higher hydrocarbons, that find many applications in chemistry, manufacturing and industry [18–23]. CO₂ hydrogenation (i.e., reduction under a pressure of hydrogen gas) is, in principle, the most atom-efficient method, but has safety risks connected with the use of flammable, pressurized gas. Alternative reductants such as hydrosilanes and hydroboranes have been successfully applied to replace H₂, as they are liquid at room temperature, hence easier and safer to handle and store. They can bring about CO₂ reduction to different products under mild reaction conditions, due to the fact that E–H bonds (E = Si, B) are weaker than the H–H bond, and that the formation of stronger E–O bonds constitutes a driving force for the reaction. It has been demonstrated that CO₂ can be reduced by a hydroborane (Scheme 1) to give formoxyborane (A), bis(boryl)acetal (B), methoxyborane (C) and bis(boryl)ether (D), and that the choice of appropriate homogeneous catalysts can drive the selectivity of the process to the desired products, further than promoting the overall reaction rate [16]. Although precious transition metals play a dominant role as catalysts for CO₂ reduction, various studies demonstrated the possible use of earth-abundant metals and p-block elements [24,25]. An excellent, comprehensive review on this chemistry was published by Bontemps in 2016 [16]. The present review summarizes the main results described in the literature since 2016 on the synthetic aspects of main group and transition metal-based homogeneous catalysts, and on the selectivity obtained in CO₂ hydroboration process. The main reaction parameters are summarized in Table 1, whereas the most diagnostic nuclear magnetic resonance (NMR) data are collected in Table 2.

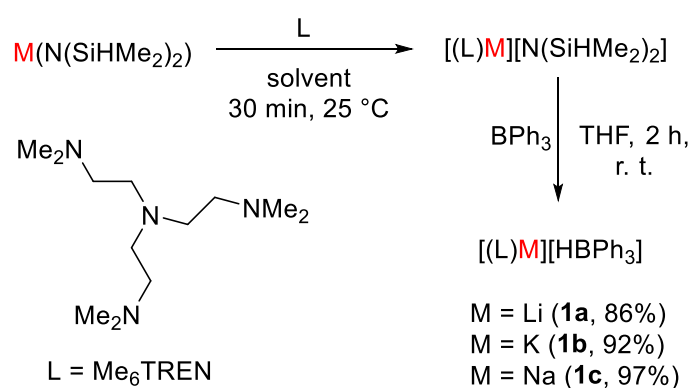
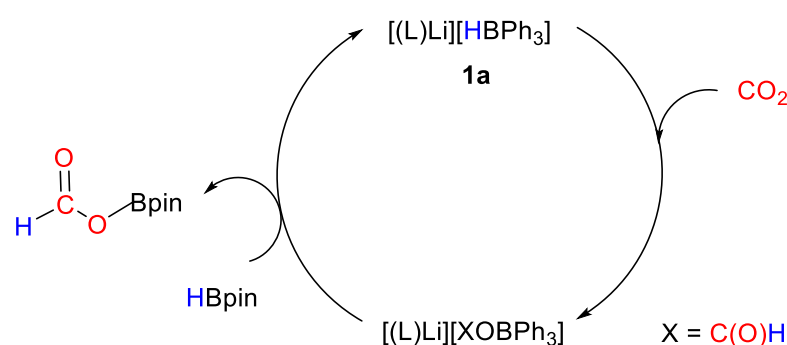


Scheme 1. General reaction and product distribution for CO₂ hydroboration.

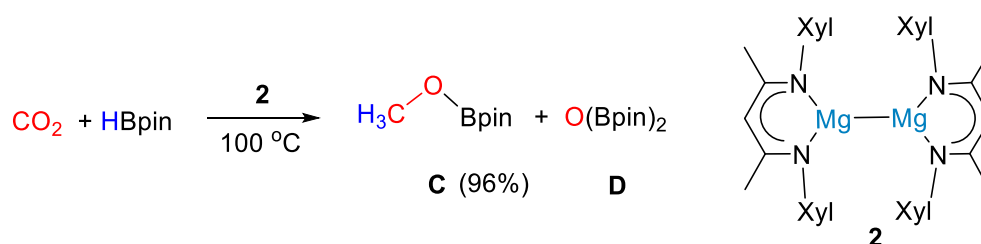
2. Main Group Metal Catalysts for CO₂ Hydroboration

Okuda and coworkers [26] showed that alkali metal hydridotriphenylborates [M(HBPh₃)] [1, M = Li (a), Na (b), K (c)] act as efficient catalysts for hydroborative reduction of CO₂ using pinacolborane (HBpin) to give formoxyborane (OCHO)Bpin. The complexes were obtained from the reaction of metal precursors [M(N(SiHMe₂)₂)] with ligand tris[2-(dimethylamino)ethyl]amine (Me₆TREN) in tetrahydrofuran (THF) or pentane (Scheme 2). The mixtures were usually stirred for 30 min at room temperature and in the next step the resulting complex was mixed with B(Ph)₃ in THF to obtain complexes of general formula [(L)M][HBPh₃], where M = Li (1a), Na (1b), K (1c). The obtained complexes were fully characterized by spectroscopic methods, such as ¹H, ¹³C, ¹¹B NMR and infrared (IR).

The catalytic reactions between CO₂ (1 atm) and HBpin (0.14 mmol) were tested in the presence of metal complexes 1a–c (1 mol%) at room temperature in THF (0.5 mL). The lithium derivative 1a gave the best result with a turnover frequency (TOF) of 10 h^{−1} (reaction time = 10 h) compared to sodium (1b, TOF = 6.25 h^{−1}, reaction time = 16 h) and potassium (1c, TOF = 6.25 h^{−1}, reaction time = 16 h) complexes. A simplified mechanism was proposed (Scheme 3) based on stoichiometric reactions with CO₂ and HBpin, showing that CO₂ activation occurs by insertion into the H–B bond in the anion of 1. The so-obtained formoxytriphenylborate complexes [(L)M{(HCO₂)BPh₃}] [1, M = Li (a); Na (b); K (c)] were fully characterized by ¹H, ¹³C, ²⁹Si NMR and infrared spectroscopy (Table 2). Mechanistic and computational studies were planned at the time of publication [26].

Scheme 2. Synthetic routes to **1a–c** [26].Scheme 3. Proposed mechanism for CO_2 hydroboration with **1a** [26].

The low-valent magnesium(I) complex $[(^{Xyl}Nacnac)Mg]_2$ (**2**, $Xyl = 2,6-Me_2C_6H_3$) was employed by Ma and coworkers [27] as a highly efficient precatalyst for the hydroboration of CO_2 under mild conditions. Complex **2** (Scheme 4) was synthesized from reaction of precursor $[MgI(OEt_2)(Nacnac)]$ with an excess of potassium metal in toluene over 24 h.

Scheme 4. CO_2 hydroboration in the presence of complex **2** [27].

The reaction between HBpin (0.5 mmol) and carbon dioxide (1 bar) led to methoxyborane in high yields (96%) using 5 mol% of **2** at 100 °C for 15 h (Scheme 4). Although a reaction mechanism was not proposed, stoichiometric reactions between **2** and HBpin showed that hydroborane activation led to the dimeric magnesium boryloxide complex $[(^{Xyl}Nacnac)Mg(\mu-OBpin)]_2$ (**2a**, Figure 2), and this was proposed as a catalytic intermediate [27].

The magnesium bis(hydridotriphenylborate) complex $[Mg(thf)_6][HBPh_3]_2$ (**3**) was synthesized by Okuda and coworkers and briefly investigated as catalyst for CO_2 hydroboration under ambient conditions (10 mol% catalyst, THF- d_8 , 25 °C, 3 h) [28]. It was isolated as a solvent-separated ion pair from the reaction of $[Mg\{N(SiHMe_2)_2\}_2]$ with BPh_3 in THF for 12 h at room temperature (Scheme 5).

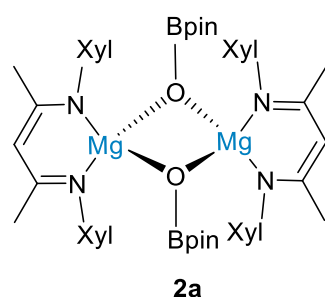
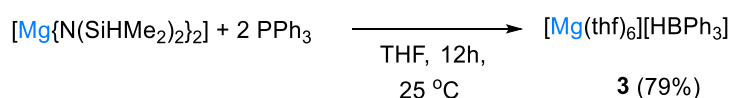
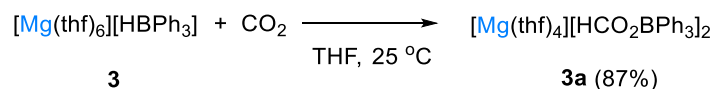


Figure 2. Drawing of complex **2a** [27].



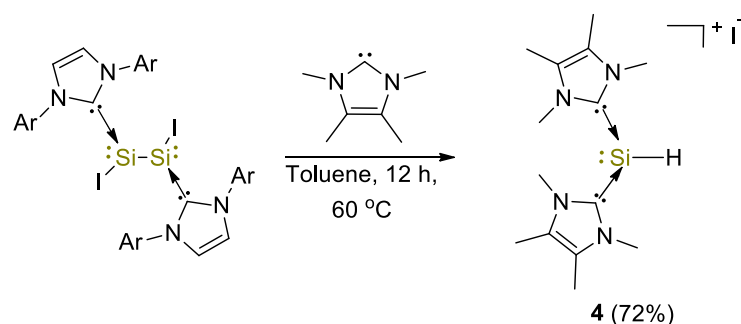
Scheme 5. Synthesis of complex **3** [28].

With HBpin, complex **3** gave a 1:1 mixture of CH₃OBpin and pinBOBpin, whereas the alkali metal hydridoborates [(L)M][HBPh₃] and the metal-free ammonium salt [ⁿBu₄N][HBPh₃] selectively gave the formoxyborane (OCHO)Bpin. Although the authors did not give full mechanistic details, it was shown that rapid CO₂ insertion into the B–H bond of **3** gave the bis(formoxytriphenylborate) complex [Mg(thf)₄][HCO₂BPh₃]₂ (**3a**) in high yield (Scheme 6). Complex **3a** showed a characteristic chemical shift at 2.9 ppm in DMSO-d₆ in the corresponding ¹¹B NMR spectrum [28].



Scheme 6. Synthesis of complex [Mg(thf)₄][HCO₂BPh₃]₂ (**3a**) [28].

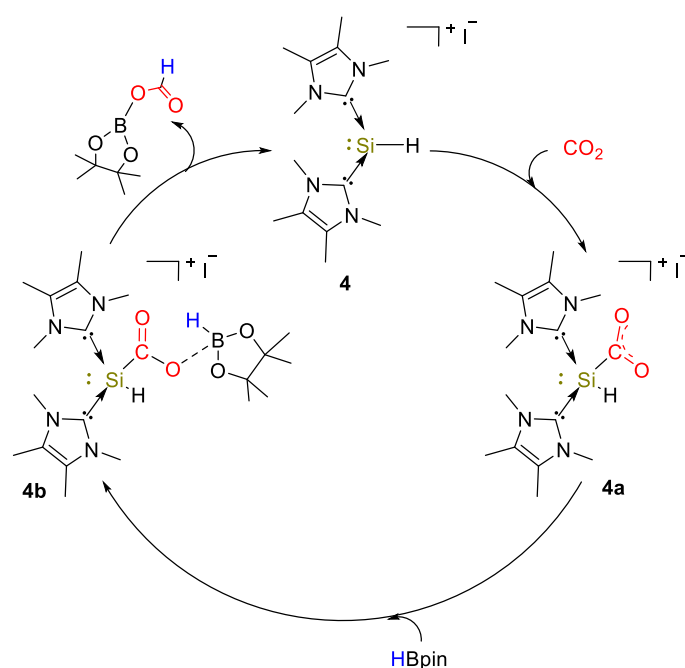
The first example of use of a silicon(II) complex for the hydroboration of CO₂ was described by So and coworkers [29]. The NHC-stabilized silyliumylidene cationic complex [(I^{Me})₂SiH]I (**4**, I^{Me} = :C{N(Me)C(Me)}₂) was obtained from the reaction between the NHC-iodosilicon dimer [I_{Ar}(I)Si]₂ (where I_{Ar} = :C{N(Ar)CH}₂) with four equivalents of I^{Me} in toluene at 60 °C (Scheme 7). The complex was fully characterized by spectroscopic methods such as IR and UV–Vis spectroscopy and ¹H, ²⁹Si NMR, giving signals at 9.73 ppm for the Si–H bond and –77.9 ppm (¹J_{SiH} = 283 Hz), respectively [30].



Scheme 7. Synthesis of complex **4** [29].

Complex **4** was used as an efficient catalyst (10 mol%) for the selective reduction of CO₂ with HBpin to formoxyborane (OCHO)Bpin, in details reaching a yield of 94% after 0.08 h (TOF = 113.2 h^{−1}). After 0.17 h complete conversion was observed, with 98% of (OCHO)Bpin (TOF = 58.7 h^{−1}) and 2% of (Bpin)O(Bpin) under 90 °C. At lower catalyst loadings (5 mol%), the catalytic hydroboration was incomplete (90% conversion

to (OCHO)Bpin, 0.5 h). $\text{BH}_3\cdot\text{S}(\text{Me})_2$ was also tested and the borate $\text{B}(\text{OMe})_3$ (18%) and $[\text{BO}(\text{OMe})_3]$ (81%) were observed as products in 1:4 ratio after 0.5 h ($\text{TOF} = 19.8 \text{ h}^{-1}$). The hydroboration of CO_2 using catecholborane (HBcat) needed longer reaction times (24 h, >99% conversion, $\text{TOF} = 0.34 \text{ h}^{-1}$) to afford a mixture of bis(boryl)ether (Bcat) $_2\text{O}$ (major product, yield = 70%) and methoxyborane CH_3OBcat (minor product, yield = 12%). Density functional theory (DFT) calculations and NMR experiments led to the proposed mechanism shown in Scheme 8. Further studies showed that by reacting **4** with excess HBpin in C_6D_6 at 60 °C for 5 min, a ^{11}B NMR signal at 0.92 ppm was observed, whereas the ^1H NMR spectrum showed a set of signals due to methyl protons of IMe and Bpin. The ^{29}Si NMR spectrum displayed a singlet at -93.0 ppm, corresponding to a Si(II) cationic center. The authors attributed these signals to the NHC-borylsilyliumylidene complex $[(\text{IMe})_2\text{Si}(\text{Bpin})]\text{I}$ that tested as catalyst (2.5 mol%) gave (OCHO)Bpin in 94% yield after 0.17 h, corresponding to a TOF of 227 h^{-1} [29].

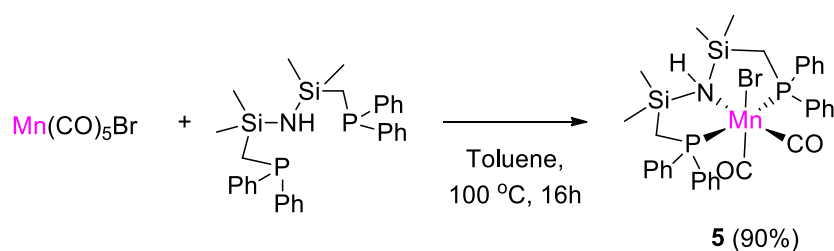


Scheme 8. Proposed mechanism for CO_2 hydroboration with **4** [29].

In summary, main group metal (Li, Na, K, Mg) and non-metal (Si) compounds and adducts showed a modest degree of activity for CO_2 hydroboration, using hydroboranes such as pinacolborane (HBpin), catecholborane (HBcat) and 9-BBN, under mild reaction conditions. Whereas alkali metals did not play a role in either borane or CO_2 activation, the role of the Mg(II) centers in the activation mechanism likely depended on the nature of the complex, and in the case of **2**, borane activation seems to take place first. On the other hand, Si(II)-NHC hydrido adducts were proposed to activate preferentially CO_2 , which then reacts with HBpin in an outer-sphere fashion, to give formoxyborane as product. The process selectivity varied from formoxy- to methoxyborane products, and the latter are generally obtained at higher temperature (90–100 °C, Table 1).

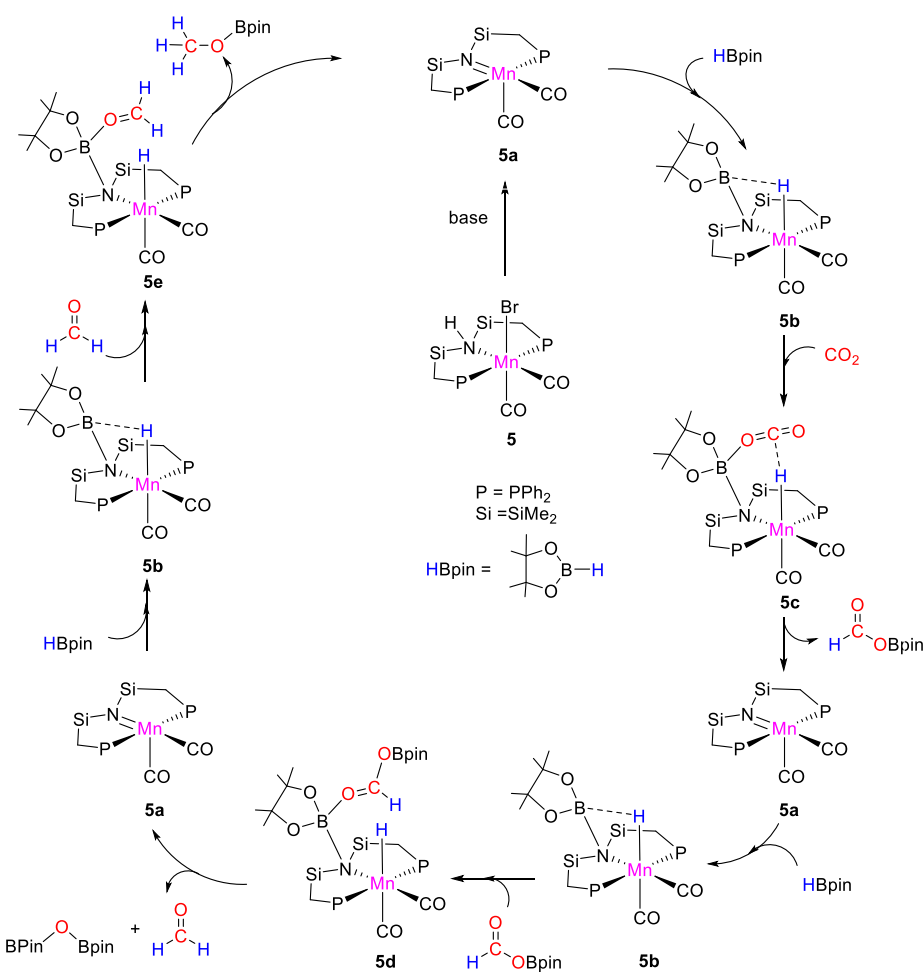
3. First-Row Transition Metal Catalysts for CO_2 Hydroboration

The first example of use of a manganese complex in CO_2 hydroboration was reported by Leitner and coworkers [31]. The complex $[\text{MnBr}\{(\text{Ph}_2\text{PCH}_2\text{SiMe}_2)_2\text{NH}\}(\text{CO})_2]$ (**5**) was synthesized in 90% yield by treatment of $[\text{Mn}(\text{CO})_5\text{Br}]$ with 1,3-bis((diphenylphosphino)methyl)tetramethyldisilazane in toluene at 100 °C for 16 h (Scheme 9). The product was characterized by ^1H , ^{13}C , ^{31}P NMR and single crystal X-ray diffraction analysis in the solid state. The $^{31}\text{P}\{^1\text{H}\}$ NMR spectrum of **5** showed a singlet at 48.46 ppm, downfield shifted from the value of -22.51 ppm of the free ligand, as expected upon coordination to the metal center [31].



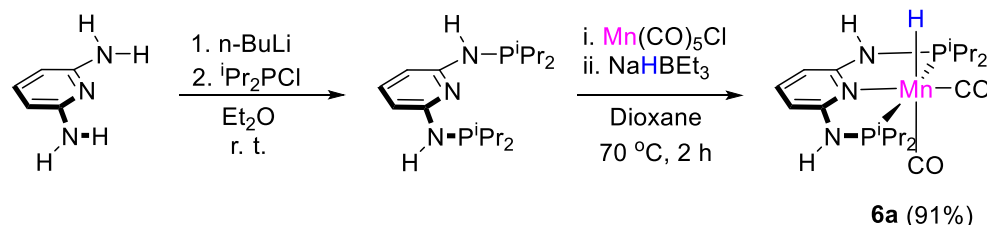
Scheme 9. Synthesis of complex **5** [31].

Complex **5** catalyzed the selective formation of methoxyborane from carbon dioxide hydroboration with HBpin under mild conditions (CO_2 , 1 atm; $[\text{Mn}]$ 0.072 mol%; NaO^tBu , 0.2 mol%; HBpin, 2.76 mmol; 90 °C; 14 h). Control experiments demonstrated that both the Mn complex and the base were required. The best results in terms of Turnover Numbers (TON = 883) were obtained at 100 °C, under solvent-free conditions. A proposed mechanism was described (Scheme 10). In the presence of base, **5** is converted to the active Mn-imino species **5a**. Pinacolborane is activated through B–N bond formation generating **5b**, which reacts with CO_2 to give intermediate **5c**, from which formoxyborane (OCHO)Bpin is released regenerating **5a**. The second reduction step involves the activation of (OCHO)Bpin by **5b** to give the manganese-acetal species **5d**. This species in turn releases formaldehyde and pinBOBpin giving back **5a**. The third step involves the activation of formaldehyde again by **5b**, followed by release of the desired product CH_3OBpin and **5a** [31].



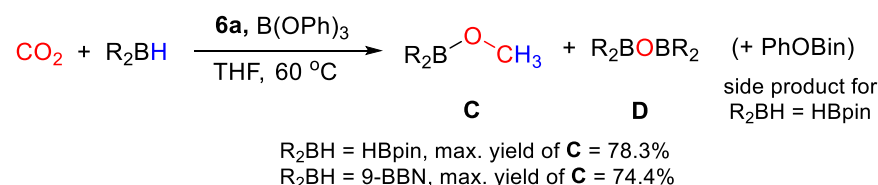
Scheme 10. Proposed mechanism for CO_2 hydroboration with **5** [31].

Gonsalvi, Kirchner and coworkers [32] tested the well-defined manganese complexes $[\text{MnH}(\text{PNP}^{\text{NR}^i\text{Pr}})(\text{CO})_2]$ [6, R = H (a), Me (b)] for the selective reduction of CO_2 to methoxyboranes using HBpin and 9-BBN (9-BBN = 9-borabicyclo[3.3.1]nonane) and borates as Lewis acids additives. Complex **6a** was previously synthesized by Kirchner and coworkers in 91% yield by reaction of PNP^iPr and $\text{Mn}(\text{CO})_5\text{Cl}$ in dioxane, for 2 h at 70°C , followed by reaction of the halide product with NaHBET_3 (Scheme 11) [33].



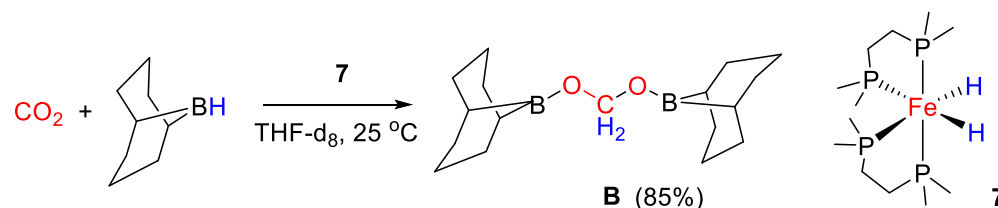
Scheme 11. Synthesis of complex **6a** [32].

In the catalytic study, it was observed that the choice of solvent was crucial to drive the selectivity of the process to the desired six-electrons reduction product. High yields in CH_3OBpin (up to 78%) were obtained after 24 h of reaction in THF-d_8 under mild reaction conditions (1 bar CO_2 , 60°C) using **6a** (2.24×10^{-3} mmol, 1 mol% to HBpin), and $\text{B}(\text{OPh})_3$ as co-catalyst (2.24×10^{-2} mmol) (Scheme 12). On the other hand, $(\text{OCHO})\text{Bpin}$ was obtained with yields as high as 73% running the tests under the same conditions using DMSO-d_6 as solvent. A side product, derived from unproductive reaction of HBpin with $\text{B}(\text{OPh})_3$, was identified as $(\text{PhO})\text{Bpin}$ by ^{11}B NMR spectroscopy. Using $(9\text{-BBN})_2$, a maximum yield in $\text{CH}_3\text{O}(9\text{-BBN})$ of 74.4% was obtained. Preliminary mechanistic studies suggest that the initial activation step may occur by cationization of the metal center by the strong Lewis acid, and that both metal-catalyzed and metal-free steps may be present [33].



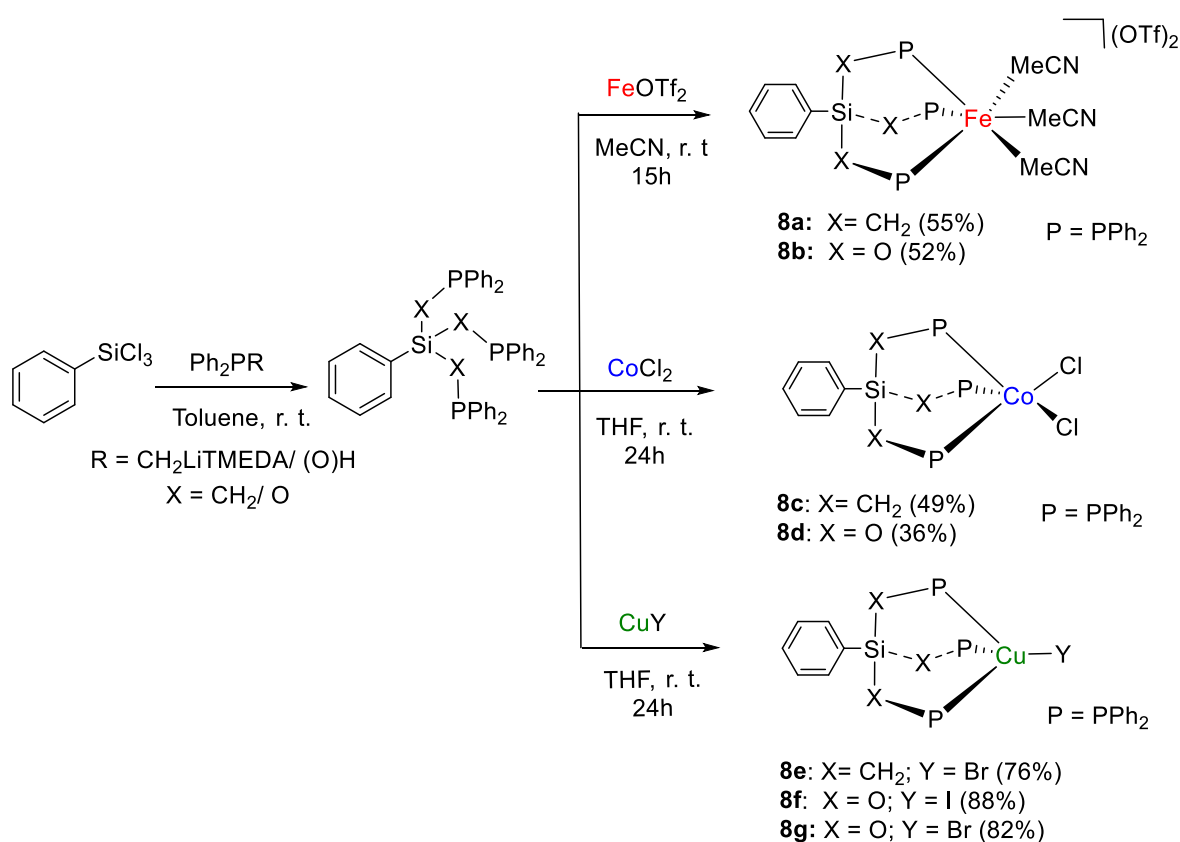
Scheme 12. CO_2 hydroboration in the presence of complex **6a** [33].

Bontemps and coworkers [34] applied the iron(II) bis(hydrido) complex $\text{cis-}[\text{Fe}(\text{H})_2(\text{dmpe})_2]$ [7, dmpe = 1,2-bis(dimethylphosphino)ethane] for the reduction of CO_2 with 9-BBN, affording selectively the bis(boryl)acetal derivative $(9\text{-BBN})\text{OCH}_2\text{O}(9\text{-BBN})$ in 85% yield under mild conditions (25°C) and with very short reaction time (45 min) (Scheme 13). The study can be considered a breakthrough result, as this protocol represents a synthetically viable way to obtain a molecule that is potentially useful for CH_2 group transfer to various organic derivatives, giving in turn a variety of value added products and in some cases generating chiral carbon centers [34].



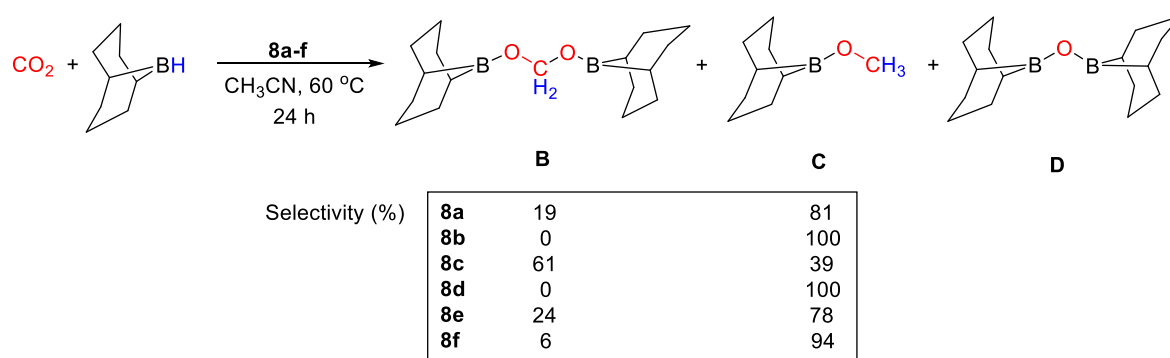
Scheme 13. CO_2 hydroboration in the presence of complex **7** [34].

The tridentate ligand-stabilized iron(II), cobalt(II) and copper(I) complexes $[\text{Fe}(\kappa^3\text{-PhSi}\{\text{CH}_2\text{PPh}_2\}_3)(\text{MeCN})_3][\text{OTf}]_2$ (**8a**, $\text{OTf} = \text{O}_3\text{SCF}_3$), $[\text{Fe}(\kappa^3\text{-PhSi}\{\text{OPPh}_2\}_3)(\text{MeCN})_3][\text{OTf}]_2$ (**8b**), $[\text{Co}(\kappa^2\text{-PhSi}\{\text{CH}_2\text{PPh}_2\}_3)\text{Cl}_2]$ (**8c**), $[\text{Co}(\kappa^3\text{-PhSi}\{\text{OPPh}_2\}_3)\text{Cl}_2]$ (**8d**), $[\text{Cu}(\kappa^3\text{-PhSi}\{\text{CH}_2\text{PPh}_2\}_3)\text{Br}]$ (**8e**), $[\text{Cu}(\kappa^3\text{-PhSi}\{\text{OPPh}_2\}_3)\text{I}]$ (**8f**) and $[\text{Cu}(\kappa^3\text{-PhSi}\{\text{OPPh}_2\}_3)\text{Br}]$ (**8g**), prepared by complexation of metal salt precursors according to Scheme 14, were shown by Cantat and coworkers to promote the catalytic hydroboration of CO_2 with $(9\text{-BBN})_2$ [35]. Diagnostic $^{31}\text{P}\{^1\text{H}\}$ NMR signals fall in a broad range of chemical shifts, depending on the ligand and metal. For example, **8a** is characterized by a singlet at 30.15 ppm, whereas the phosphinite analogue **8b** shows a singlet at 147.93 ppm in CD_3CN . As expected, it was not possible to collect $^{31}\text{P}\{^1\text{H}\}$ NMR spectra for the Co(II) complexes **8c,d** due to paramagnetism. For **8e**, a multiplet at ca. -33 ppm ($J_{\text{P-63Cu}} \sim 840$ Hz, $J_{\text{P-65Cu}} \sim 900$ Hz) was observed in CD_2Cl_2 , instead signals at 80 ppm (m, $J_{\text{P-Cu}} \sim 860$ Hz, CD_2Cl_2) and 82.9 ppm (brs, C_6D_6) were identified for **8f** and **8g**, respectively.



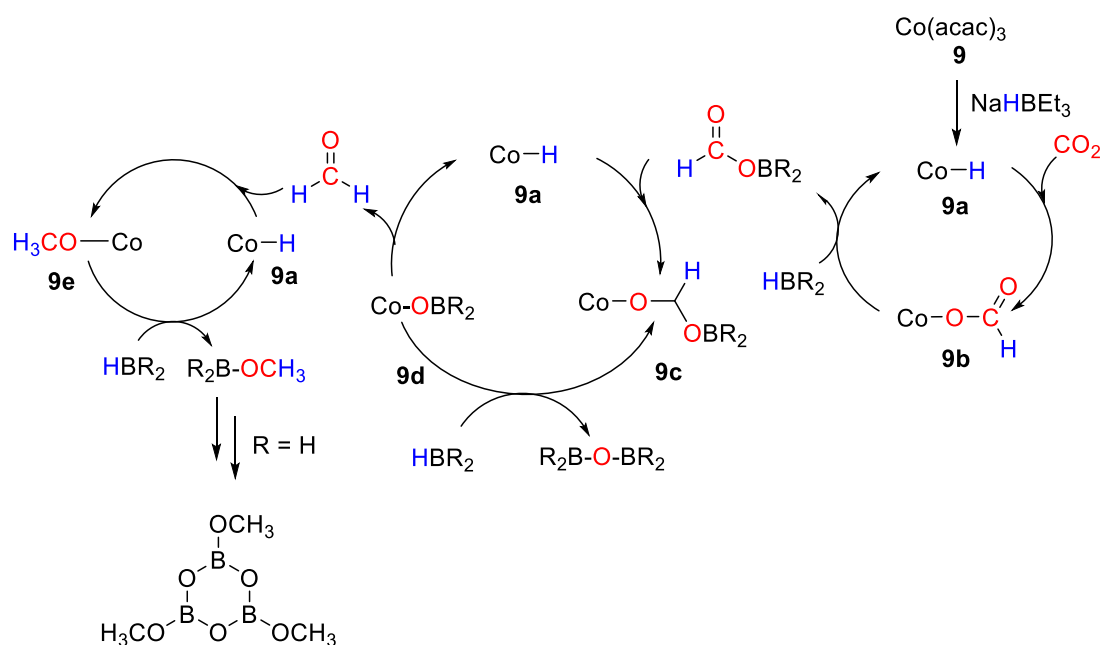
Scheme 14. Synthetic routes to **8a–g** [35].

In the case of Fe(II) and Co(II) complexes, those stabilized by $\text{PhSi}(\text{CH}_2\text{PPh}_2)_3$ showed higher activities than those containing $\text{PhSi}(\text{OPPh}_2)_3$, whereas the reverse trend was observed with the Cu(I) complexes. Remarkably, both copper catalysts **8e** and **8f** favor the reduction of CO_2 to the acetal derivatives. Quantitative conversion of $(9\text{-BBN})_2$ into a 4:1 mixture of $(9\text{-BBN})\text{OCH}_2\text{O}(9\text{-BBN})_2$ and $\text{CH}_3\text{O}(9\text{-BBN})$ was obtained at room temperature. The best TON = 66 was achieved with complex **8f**. The iron and cobalt catalysts showed lower activities, giving preferentially $\text{CH}_3\text{O}(9\text{-BBN})$ at 60°C . The authors suggested that the copper complexes act as Lewis acids and their catalytic activity may become enhanced upon coordination to the less electron donating ligand. The product distributions and selectivities obtained for each system are shown in Scheme 15 [35].



Scheme 15. CO₂ hydroboration in the presence of complex **8a–f** [35].

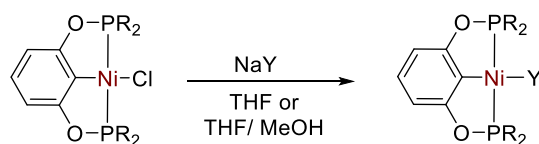
An effective and efficient reduction of CO₂ by different hydroboranes into methoxyboranes was disclosed by Tamang and Findlater [36], using Co(acac)₃ (**9**) as pre-catalyst. With BH₃·S(Me)₂, CO₂ hydroboration gave [BO(OMe)]₃ as product. Sluggish reactions were observed with HBCat, giving a maximum 25% of CH₃OBcat after 72 h. The reaction with pinacolborane gave mixture of products: formoxyborane (27%), bis(boryl) ether (63%) and methoxyborane (4%), reaching maximum TON = 300 and TOF = 15 h⁻¹. The mechanism shown in Scheme 16 was proposed for CO₂ hydroboration in the presence of **9**. The addition of NaHBET₃ to a solution of [Co(acac)₃] leads at first to the formation of the active Co–H species (**9a**). Next, the insertion of CO₂ into the Co–H bond generates the cobalt formate complex **9b**. Subsequent transmetalation of the formate complex using HBR₂ provides formoxyborane and regeneration of **9a**. Insertion of formoxyborane into the Co–H bond of **9a** gives the metal acetoxy complex **9c**, which can undergo β-alkoxy elimination to generate free formaldehyde and the metal alkoxyborane **9d**. Insertion of free formaldehyde into the Co–H bond of **9a** gives the methoxy cobalt complex **9e** from which methoxyborane is finally released [36].



Scheme 16. Proposed mechanism for CO₂ hydroboration with **9** [36].

Chen and coworkers [37,38] described a number of different types of bis(phosphinite) POCOP-type Ni(II) pincer complexes of general formula [{2,6-(R₂PO)₂C₆H₃}NiX] (R = ^tBu, ⁱPr, Ph; X = SH, N₃, NCS, SC₆H₄-p-OCH₃, SC₆H₄-p-CH₃, SC₆H₅, SC₆H₄-p-CF₃, SCH₂C₆H₅)

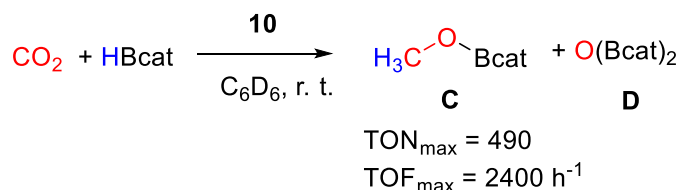
(Scheme 17), that were applied for the catalytic hydroboration of CO₂ in the presence of HBcat.



Y = SH, NCS, SC₆H₄-p-OCH₃ (**10a**), SC₆H₄-p-CH₃,
SC₆H₅, C₆H₄-p-CF₃, SCH₂C₆H₅; R = ⁱBu; ⁱPr
Y = N₃; R = ⁱPr (**10b**)

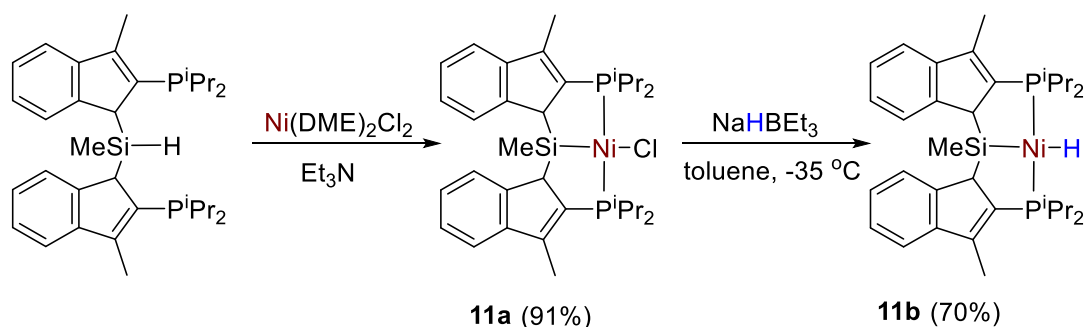
Scheme 17. Synthesis of complexes [2,6-(R₂PO)₂C₆H₃]NiX [37,38].

It was found that pincer complexes with ⁱPr₂P phosphine arms are more active than those with ⁱBu₂P arms, whereas those with Ph substituents decomposed. The reduction proceeds to the methoxyborane (CH₃O-Bcat) level (Scheme 18), reaching a maximum TON = 490 and TOF = 2400 h⁻¹ at room temperature under an atmospheric pressure of CO₂ with 0.2 mol% of the thiolato complex [2,6-(ⁱBu₂PO)₂C₆H₃]Ni(SC₆H₄-p-OCH₃) (**10a**) [38]. The best results for the other series of complexes, containing non-thiolato Y ligands, were obtained with pre-catalyst [2,6-(ⁱPr₂PO)₂C₆H₃]NiN₃ (**10b**, TON = 477, TOF = 1908 h⁻¹). The catalytic activity follows the series X = SH ≈ N₃ >> NCS). The authors propose that the nickel hydride complex [2,6-(R₂PO)₂C₆H₃]NiH is the active catalyst, generated in situ in all cases [37].



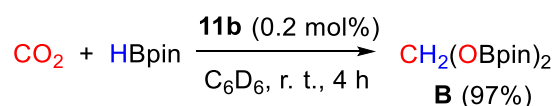
Scheme 18. CO₂ hydroboration in the presence of complex **10** [37].

The synthesis and characterization of Ni-Cl (**11a**) and Ni-H (**11b**) pincer complexes supported by a new bis(indolylphosphino)silyl ligand (Scheme 19) was described by Turculet and coworkers [39]. All complexes were fully characterized by spectroscopic methods (¹H, ¹³C, ³¹P, ²⁹Si NMR). Complex **11a** featured a ³¹P{¹H} NMR signal a 36.0 ppm (s, C₆D₆) and a ²⁹Si NMR singlet at 43.8 ppm. The hydride derivative **11b** instead showed a ³¹P{¹H} NMR signal at 65.6 ppm, and a ²⁹Si NMR signal at 59.8 ppm. The corresponding Ni-H resonance showed to be temperature-dependent, featuring a broad hydride resonance at -4.80 ppm at room temperature. At low temperature (-60 °C, toluene-d₈) this signal is resolved into an apparent triplet with ²J_{PH} = 47 Hz.



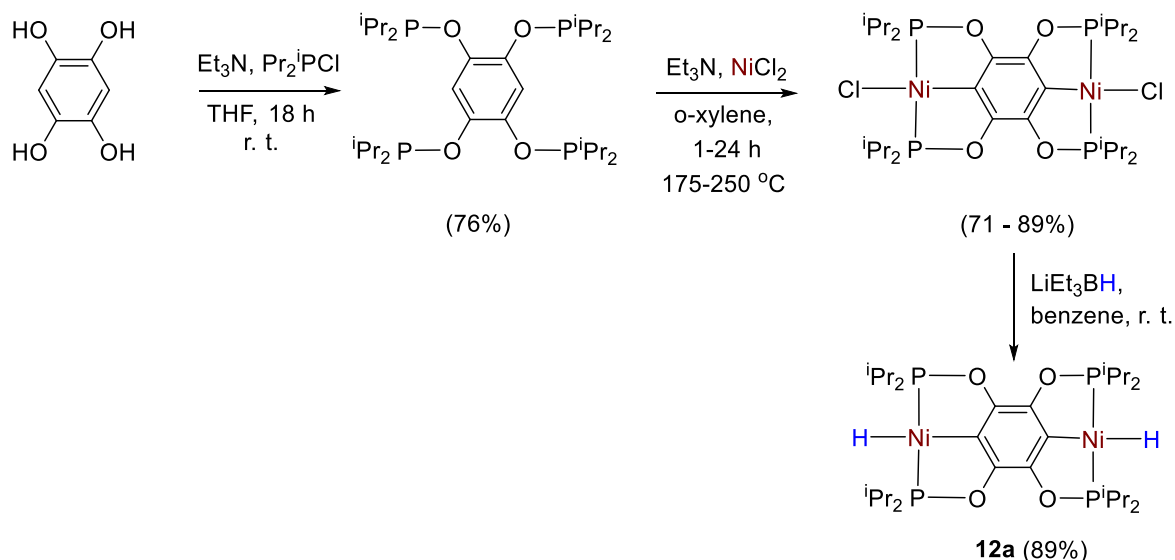
Scheme 19. Synthetic routes to **11a,b** [39].

The nickel hydride complex (**11b**) exhibited unprecedented selectivity (97%) for the hydroboration of CO₂ with HBpin to the formaldehyde level, giving the bis(boryl)acetal CH₂(OBpin)₂ in high yields under mild conditions (25 °C, 4 h, 0.2 mol% of **11b**, Scheme 20). The bis(boryl)acetal was successfully isolated and applied as a source of methylene for the formation of C–N and C–P bonds. Although a rationale for this high selectivity to acetal was not given, stoichiometric experiments showed that CO₂ activation initially occurs by insertion into the Ni–H bond to give the corresponding formato complex [39].



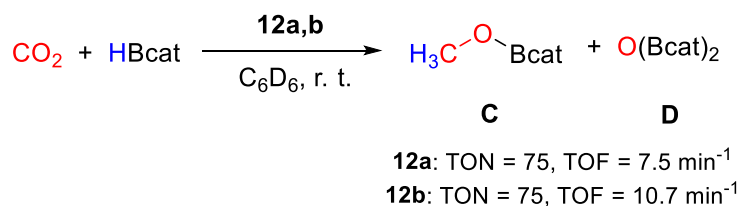
Scheme 20. CO₂ hydroboration in the presence of complex **11b** [39].

Guan and coworkers [40] applied the phosphinite-based homobimetallic nickel pincer complex [(2,3,5,6-(ⁱPr₂PO)₄C₆)Ni₂H₂] (**12a**) as catalyst for CO₂ hydroboration. Complex **12a** was synthesized in a two steps reaction. In the first step, [(L)Ni₂Cl₂] was prepared either by heating a mixture of 1,2,4,5-tetrahydroxybenzene, ⁱPr₂P–Cl, NiCl₂ and Et₃N at 150 °C in a microwave reactor or by refluxing a mixture consisting of L = 1,2,4,5-(ⁱPr₂PO)₄C₆H₂ with NiCl₂ and Et₃N at 175–250 °C in a flask. Subsequently, halide–hydride exchange was achieved by reacting the chloride derivative with LiEt₃BH to give **12a** in ca. 89% yield (Scheme 21). The catalytic activity of **12a** was compared to that of the mononuclear analogue [(2,6-(ⁱPr₂PO)₂C₆H₃)NiH] (**12b**).



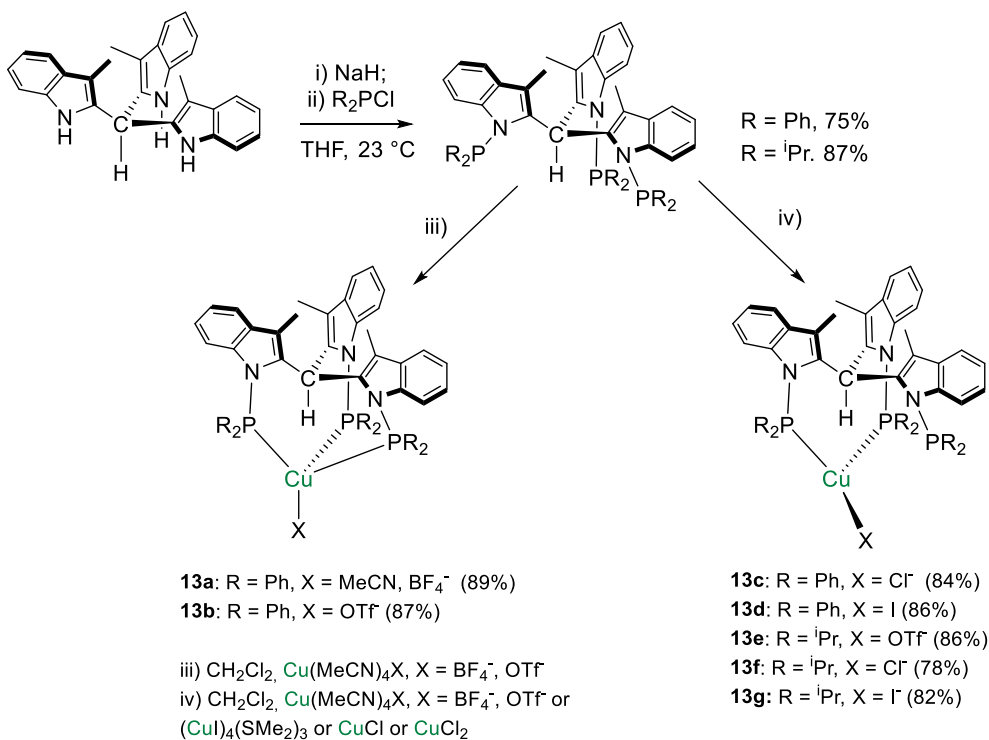
Scheme 21. Synthetic route to **12a** [40].

In the reduction of CO₂ with HBcat (100 equiv.) in C₆D₆ at 25 °C (Scheme 22), both complexes yield CH₃OBcat and catBOBcat as products. TON, based on B–H bond utilization, was measured as 75 over 10 min for **12a** (TOF = 7.5 min^{−1}), whereas **12b** showed a slightly higher efficiency (TON = 75 in 7 min, TOF = 10.7 min^{−1}). The lower efficiency of **12a** was attributed to less favorable thermodynamics for the first CO₂ insertion step and to the disfavorable entropic factor due to the bimetallic nature of **12a**. Extensive catalyst decomposition was observed at the end of the catalytic tests for both systems, hampering mechanistic investigations [40].



Scheme 22. CO₂ hydroboration in the presence of complex **12a,b** [40].

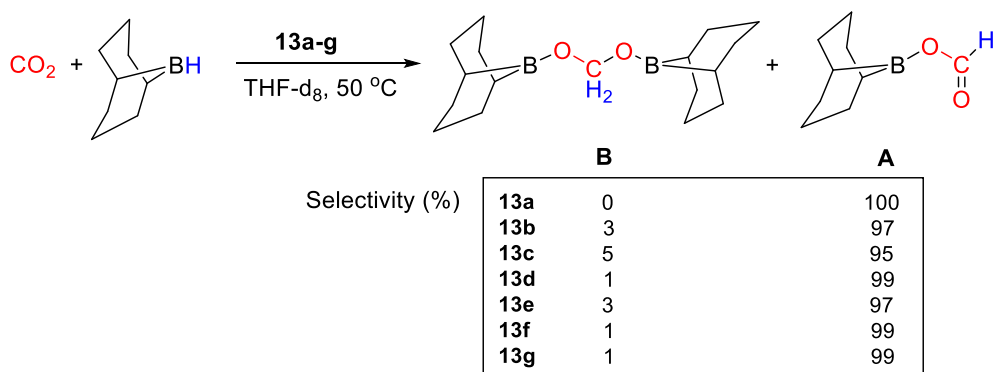
The ligands tris[1-(di-R-phosphino)-3-methyl-1H-indol-2-yl]methane (HTIM(PR₂)₃, R = Ph, ⁱPr) were used by Lloret-Fillol and coworkers [41] to coordinate Cu(I). A small library of eight Cu complexes of general formula [Cu{HTIM(PR₂)₃}X] (R = Ph, ⁱPr; X = Cl⁻, I⁻, OTf⁻, BF₄⁻) showed in Scheme 23 were obtained. Interestingly, depending on the reaction conditions, both κ³-P (**13a,b**) and κ²-P (**13c–g**) complexes were obtained in the solid state as determined by X-ray diffraction analysis. In solution, a dynamic κ³- to κ²-coordination shift was observed.



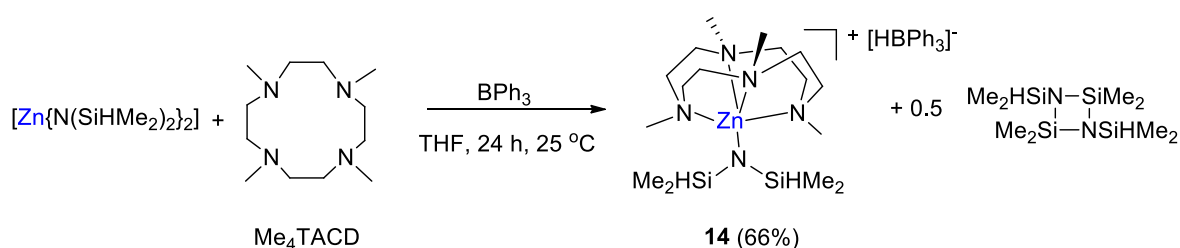
Scheme 23. Synthetic routes to [HTIM(PR₂)₃CuX] [41].

All complexes were tested as catalysts (2 mol%) for CO₂ hydroboration using (9-BBN)₂ in THF-d₈, 50 °C, 18 h. The reactions gave (OCHO)(9-BBN) as main product, with selectivities ranging from 95 to 100% (Scheme 24). Moderate TON values were measured in the range 19–31. The best results (TON = 31) were obtained with [Cu{HTIM(PR₂)₃}X] (**13g**, R = ⁱPr; X = I⁻) [41].

The zinc hydridotriphenylborate [Zn(L){N(SiHMe₂)₂}] [HBPh₃] (**14**, L = 1,4,7,10-tetramethyl-1,4,7,10-tetraazacyclododecane, Me₄TACD) was synthesized by Okuda and coworkers [42] from the reaction of [Zn{N(SiHMe₂)₂]₂ with L and BPh₃ in 1:1:2 ratio in THF for 24 h at room temperature. Complex **14** was obtained as colorless microcrystals in 66% yield (Scheme 25).

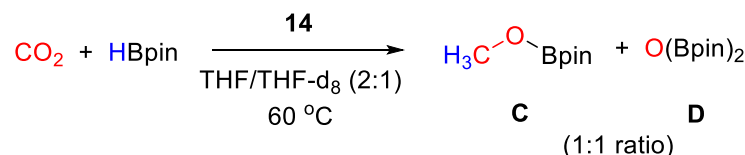


Scheme 24. CO₂ hydroboration in the presence of complexes 13a–g [41].



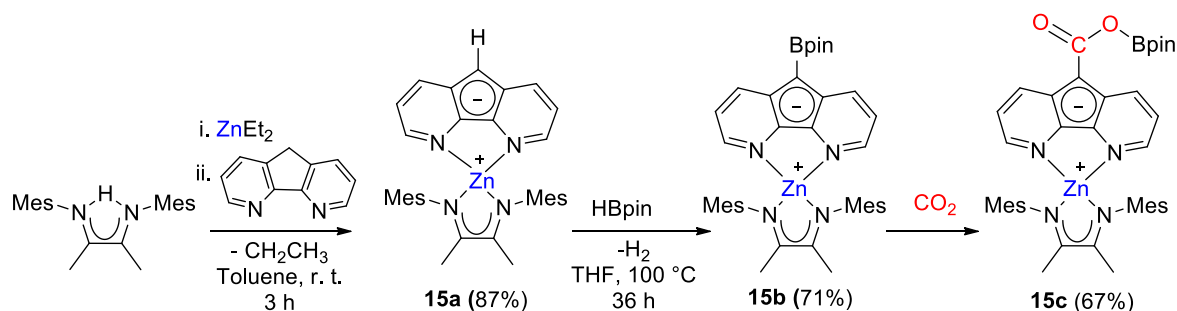
Scheme 25. Synthetic routes to 14 [42].

CO₂ hydroboration in the presence of HBpin and complex 14 (10 mol% to HBpin) was accomplished with complete conversion within 16 h at 60 °C giving a 1:1 mixture of CH₃OBpin and (Bpin)₂O (Scheme 26). It was demonstrated that CO₂ rapidly inserts into the anion B–H bond to give [Zn(L){N(SiHMe₂)₂}][(OCHO)BPh₃]. Under catalytic conditions, it is likely that further reduction occurs at the anion, to release CH₃OBpin [42].



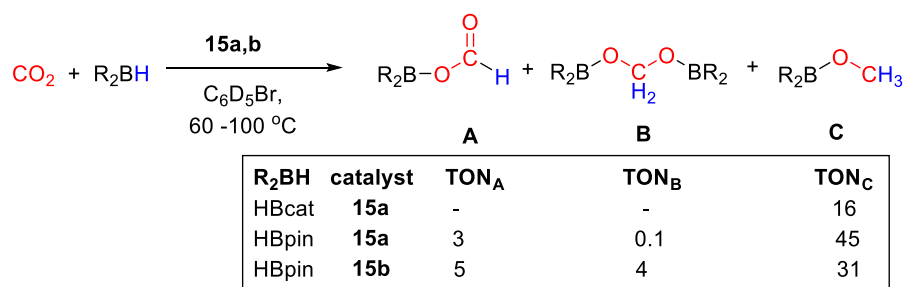
Scheme 26. CO₂ hydroboration in the presence of complex 14 [42].

Zn diazafluorenyl complexes 15a,b were synthesized by Song and coworkers [43] and tested for the catalytic reduction of CO₂ with HBCat and HBpin. [ZnL(Mes₂nacnac)] (15a, L = diazafluorenyl) was obtained from the reaction of ZnEt₂, ligand nacnac and diazafluorene in good yield. Next, 15a was reacted with HBpin to generate 15b, with formation of a new C–B bond on the diazafluorenyl moiety (Scheme 27). Stoichiometric reaction of 15b with CO₂ showed the formation of a new boronic ester derivative 15c, with insertion into the diazafluorenyl C–B bond.



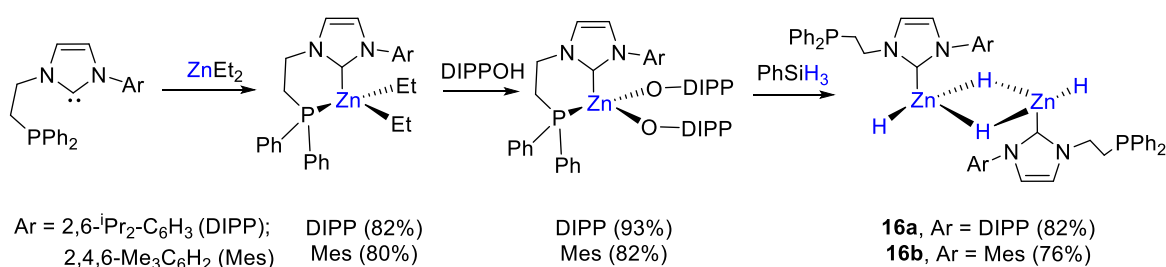
Scheme 27. Synthetic routes to 15a,b and reactivity with CO₂ to give 15c [43].

CO₂ hydroboration was carried out in the presence of 10 mol% of catalyst, HBpin or HBcat in C₆D₅Br (Scheme 28). The best activity was shown by **15a** at 90 °C for 20 h. The catalytic reactions gave the methoxy derivatives as a main products, albeit with moderate TONs. In the case of HBpin, CH₃OBpin was obtained with TON = 45, together with traces of bis(boryl)acetal (TON = 0.1) and small amounts of formoxyborane (TON = 3). For HBcat, CH₃OBcat was instead obtained with TON = 16 and complete selectivity, at 60 °C for 20 h [43].



Scheme 28. CO₂ hydroboration in the presence of complex **15a,b** [43].

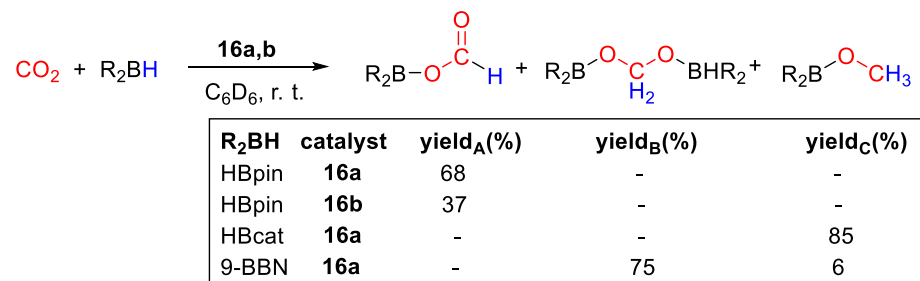
The first examples of zinc dihydrides as catalysts for the hydroboration of CO₂ was presented by Xu and coworkers [44]. The zinc complexes **16** were prepared by reaction of (P,C)-chelating ligands comprising a diphenylphosphino moiety and an Ar-NHC binding arm [Ar = 2,6-ⁱPr₂-C₆H₃ (DIPP), **a**; 1,4,6-Me₃C₆H₂ (Mes), **b**]. The first step consisted of the reaction of ZnEt₂ with an equimolar amount of ligand, to obtain the corresponding zinc dialkyl complexes. These were then converted into zinc diaryloxides by adding two equivalents of 2,6-diisopropylphenol. The last step included metathesis reactions of zinc diaryloxides with PhSiH₃ to afford the desired homobimetallic [(Zn(L)(H))₂(μ-dihydride)] complexes **16a,b** in high yields. Notably, in **16** the phosphinocarbene ligands coordinate Zn in κ¹-C fashion, with a dangling P arm (Scheme 29), as demonstrated by the ³¹P NMR resonances at −20.0 ppm (**16a**) and −19.5 ppm (**16b**), only slightly shifted from the values of the free ligands (−22.1 and −22.7 ppm, respectively). In ¹H NMR spectra, two distinct hydride signals were observed at 4.15 and 3.50 ppm for **16a** and at 4.32 and 3.46 ppm for **16b** in toluene-d₈ at −30 °C.



Scheme 29. Synthetic routes to **16a,b** [44].

Complexes **16** showed to be active catalysts for CO₂ hydroboration in C₆D₆ under very mild conditions, such as 1 bar of CO₂ and room temperature, using 0.0075 mmol of catalyst and 0.15 mmol of borane (Scheme 30). Different selectivities to products were observed, depending essentially on the type of borane used. With HBpin and **16a**, (OCHO)Bpin was obtained in 68% yield and complete selectivity under the conditions described above in a 48 h run, whereas **16b** gave the same product in 37% yield. Using **16a**, it was possible to increase the yield to 85% (12 h run) by raising the CO₂ pressure to 20 bar. Further tests using **16a** as catalysts included the use of HBcat, giving CH₃OBcat in 85% yield after 12 h with complete selectivity, and of 9-BBN, that after 4 h gave a mixture of 75% of (9-BBN)OCH₂O(9-BBN) and 6% of CH₃O(9-BBN). BH₃·S(Me)₂ gave no conversion to C1 products. The authors propose that the mechanism of CO₂ hydroboration with

16a,b follows three sequential catalytic cycles, similarly to other transition-metal hydrides. The CO₂ reduction to methanol level promoted by HBcat was attributed to its lower steric hindrance and electron richness than HBpin [44].

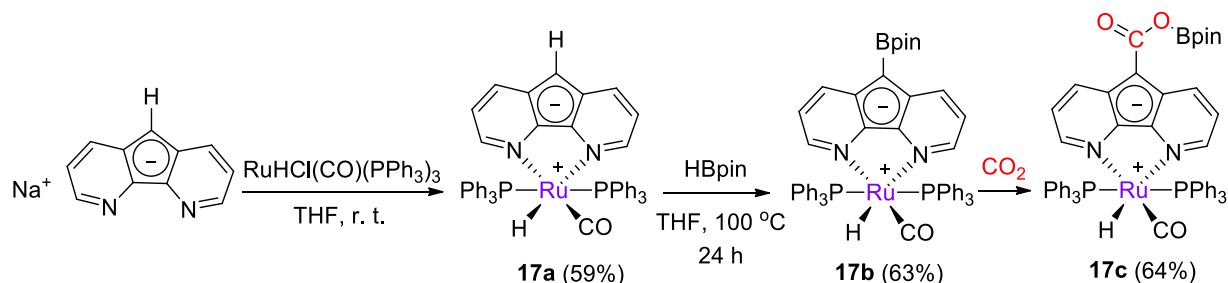


Scheme 30. CO₂ hydroboration in the presence of complex **16a,b** [44].

In summary, different first-row transition metal (Mn, Fe, Co, Ni, Cu, Zn) complexes showed to be competent catalysts for CO₂ hydroboration at different reductions levels. A wide variety of stabilizing ligands, ranging from simple bidentate bis(phosphines) such as dmpe, to tripodal triphos-type phosphine and phosphinite ligands forcing facial coordination to metal, to PNP, PCP, POCOP pincer-type, meridional ligands were applied, together with ancillary ligand-free catalytic protocols, as in the case of Co(acac)₃. Moderate to very good conversions, yields, TONs and TOFs were obtained in the different cases, with remarkable selectivities to multi-electron reductions up to the methoxy level and to the challenging acetal level. Although not all studies have reported mechanistic details, the presence of metal–hydrido bonds in the active catalysts were often invoked to explain three-step reduction pathways, starting with insertion of CO₂ into the M–H bond. The major effects in driving the selectivity of the process to a specific product were demonstrated to be more due to the steric and electronic properties of the hydroborane and to the choice of temperature and solvent rather than on the nature of the catalyst.

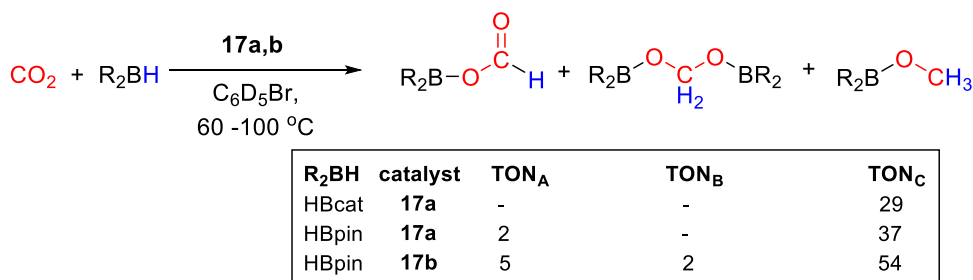
4. Second-Row Transition Metal Catalysts for CO₂ Hydroboration

Ru diazafluorenyl complexes were prepared by Song, Lei and coworkers [43] and tested for catalytic CO₂ reduction with catecholborane and pinacolborane. Complex [RuH(L)(CO)(PPh₃)₂] (**17a**) was obtained in 59% yield from the reaction of [NaL] (L[−] = diazafluorenyl) and [RuHCl(CO)(PPh₃)₃] (Scheme 31) and it was characterized by spectroscopic methods (¹H, ¹³C, ³¹P NMR). Next, **17a** was reacted with HBpin, observing the formation of the diazafluorenyl-borate derivative **17b**, with a similar reactivity of zinc complex **15a** described above. As for **15b**, the reaction of **17b** with CO₂ gave the diazafluorenyl-borate ester derivative **17c** [43].



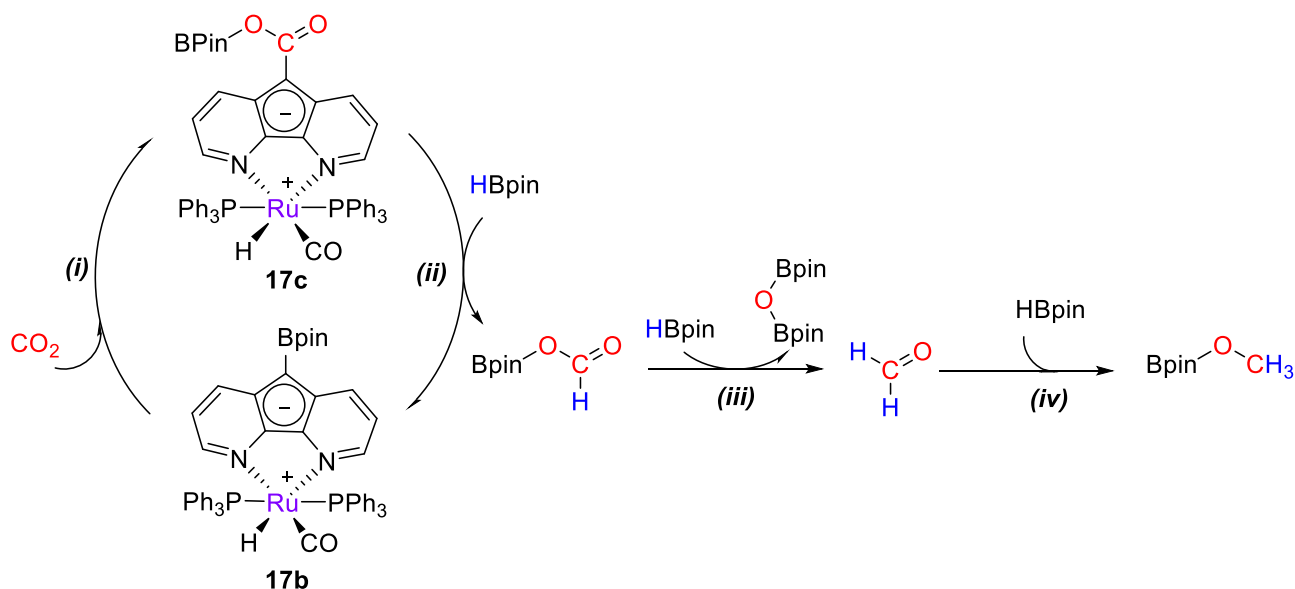
Scheme 31. Synthetic routes to **17a** and stepwise reactivity with HBpin to **17b** and CO₂ to **17c** [43].

Catalytic CO₂ hydroboration tests were run at 90–100 °C in C₆D₅Br for 45 h. In the presence of **17a** and HBcat, CH₃OBcat was obtained with TON = 29, whereas a slightly higher TON = 39 was obtained for CH₃OBpin from HBpin, together with small amounts of (OCHO)Bpin (TON = 2). In the presence of **17b**, higher productivity to CH₃OBpin was observed (TON = 54), accompanied by a higher amount of (OCHO)Bpin (TON = 5) and (Bpin)OCH₂O(Bpin) (TON = 2) (Scheme 32) [43].



Scheme 32. CO₂ hydroboration in the presence of complex **17a,b** [43].

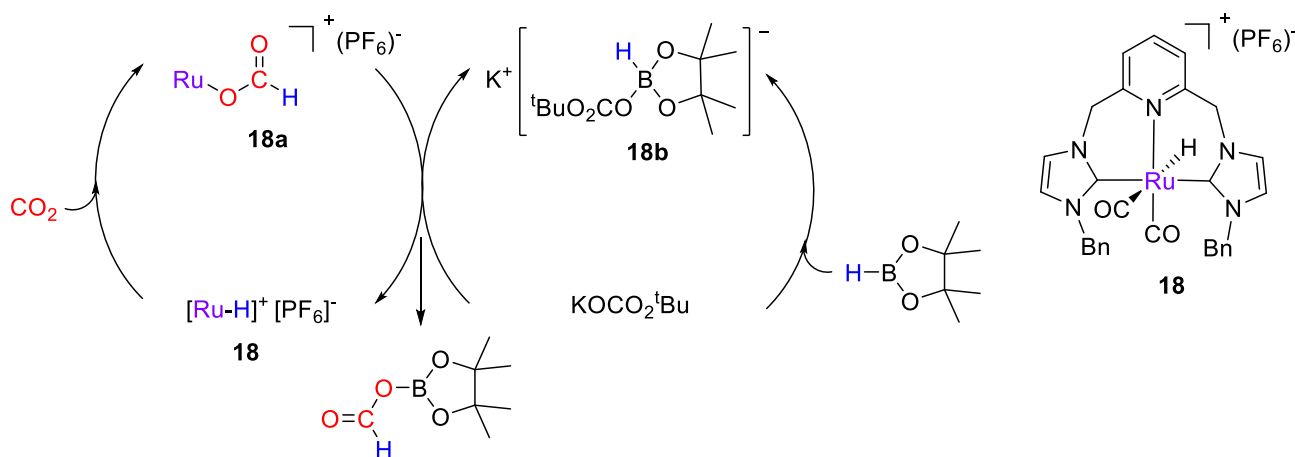
Later on, Song and Lei [45] studied the mechanism for CO₂ reduction by HBpin (Scheme 33) catalyzed by [RuH(L)(CO)(PPh₃)₂] (**17b**) through computational methods using the model complex [RuH(L)(CO)(PMe₃)₂]. The proposed hydride-shuttle mechanism consists of four steps: (i) The insertion of CO₂ into the C–B bond of **17b** to form **17c**, (ii) the reduction of **17c** to (OCHO)Bpin to regenerate **17b**, (iii) the reduction of (OCHO)Bpin to formaldehyde, and (iv) the reduction of formaldehyde to CH₃OBpin. The hydride shuttle mechanism has more accessible energy barriers than the direct bond cleavage. The σ-bond metathesis reaction of H–B and C–C bonds in stage (ii) was found to proceed through two consecutive catalytic processes involving the formation of Lewis adducts [45].



Scheme 33. Simplified mechanism for CO₂ hydroboration with **17b** [45].

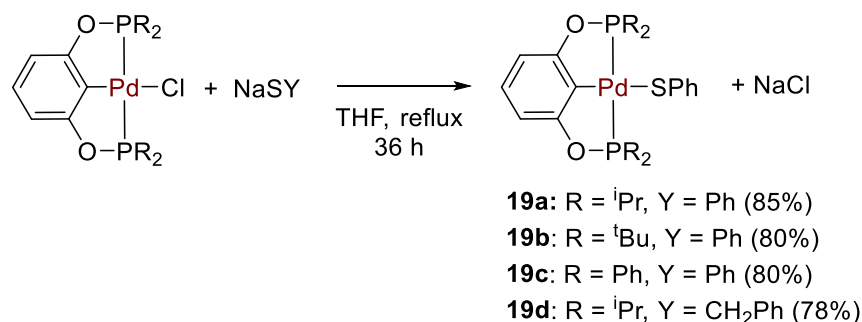
A series of cationic Ru–CNC pincer-type complexes based on 2,6-bis(NHC)pyridine were developed by Wu, Hor, Luo and coworkers [46] for selective CO₂ hydroboration, in the presence of added alkali metal salts. The catalytic tests were carried out at 25 °C in CD₂Cl₂ for 30 min using HBpin as reductant. The best results were obtained in the presence of 1 mol% of [RuH(CNC_{Bn})(CO)₂](PF₆) (**18**) and KOCO₂^tBu (2.5 mol%). The reaction gave (OCHO)Bpin in 76% yield, together with O(Bpin)₂ (10%). The proposed mechanism, based on experimental observations (Scheme 34), consists of two joint cycles (Scheme 20). Complex **18** facilitates CO₂ activation, by insertion into the Ru–H bond to give the Ru-formato inter-

mediates $[\text{Ru}(\text{CNC}_{\text{Bn}})(\text{CO})_2(\text{OCHO})]^+$ (**18a**). In the second cycle, KOCO_2^tBu reacts with HBpin to form $\text{K}[\text{Bpin}(\text{H})(\text{O}_2\text{CO}^t\text{Bu})]$ (**18b**). The authors propose the formation of a catalytically active, binary ion pair complex $[\text{Ru}(\text{CNC}(\text{CO})_2(\text{OCHO}))]^+ [{}^t\text{BuO}_2\text{CO}(\text{H})\text{Bpin}]^-$ from which $(\text{OCHO})\text{Bpin}$ is released, based on the considerations that (i) the Ru-CNC complex **18** is coordinatively saturated and, hence, has no vacant site to accommodate the coordination of HBpin ; and (ii) the catalytic data showed that in the presence of **18** but without the alkali metal salt, no activity was observed [46].



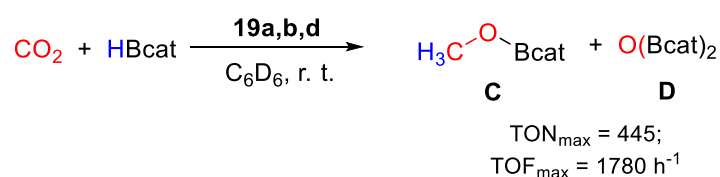
Scheme 34. Proposed mechanism for CO_2 hydroboration with **18** [46].

Palladium bis(phosphinite) POCOP pincer-type thiolate complexes **19a–d** (Scheme 35), analogues of the Ni complexes **10**, were obtained by Guan and coworkers [47] and applied as catalysts for the reduction of CO_2 with catecholborane. The complexes were synthesized from metathesis reactions of the corresponding chloride parent compounds with sodium thiolate and were characterized by multinuclear NMR and high resolution mass spectrometry (HRMS). The $^{31}\text{P}\{^1\text{H}\}$ NMR spectra showed characteristic singlets at 189.7, 192.4, 147.8 and 191.4 ppm for **19a–d**, respectively.



Scheme 35. Synthesis of Pd-POCOP complexes **19** [47].

Very high TOFs were obtained at room temperature, in benzene and under an atmospheric pressure of CO_2 with complexes **19a,b,d** (Scheme 36), whereas **19c** gave no conversion. The best results were achieved with $[\{2,6-(^i\text{Pr}_2\text{PO})_2\text{C}_6\text{H}_3\}\text{Pd}(\text{SPh})]$ (**19a**, 0.011 mmol), giving selectively CH_3OBcat with $\text{TON} = 445$, $\text{TOF} = 1780 \text{ h}^{-1}$ in a 15 min run in the presence of HBcat (5.5 mmol) [47]. Preliminary mechanistic experiments showed that by mixing **19b** with 50 equiv. of HBcat and 0.6 mL of benzene- d_6 , the $^{31}\text{P}\{^1\text{H}\}$ NMR spectrum showed only the singlet at 192.36 ppm due to **19b**. After bubbling CO_2 in the NMR tube, several new species with phosphorus resonances around 201 ppm and at 213.88 ppm were observed. The latter was attributed to the Pd hydrido complex $[\{2,6-(^t\text{Bu}^2\text{PO})_2\text{C}_6\text{H}_3\}\text{PdH}]$, that was not, however, considered as the main active species, as it gave poor results in CO_2 hydroboration than **19b** when used as a well-defined catalyst.



Scheme 36. CO₂ hydroboration in the presence of complex **19** [47].

Hazari and coworkers [48] published a detailed study showing how to drive the selectivity of Ni- and Pd-catalyzed CO₂ hydroboration to formoxyborane, bis(boryl)acetal, or methoxyborane through subtle variations of the type and concentration of the reductant, the nature and loading of the catalyst, and by addition of a Lewis acid co-catalyst. The authors synthesized a library of PCP and PSiP pincer-type Ni(II) and Pd(II) catalysts such as [(L)NiH], with L = ^{Cy}PCP (**20a**), ^{tBu}PCP (**20b**), ^{iPr}PCP (**20c**), where PCP = 2,6-C₆H₃(CH₂PR₂)₂; L = ^{Cy}PSiP (**20d**), ^{iPr}PSiP (**20e**), where PSiP = SiMe(2-PR₂-C₆H₄)₂ and [(L)PdH] with L = ^{Cy}PCP (**20f**), ^{tBu}PCP (**20g**), ^{iPr}PCP (**20h**), ^{Cy}PSiP (**20i**), ^{iPr}PSiP (**20j**) (Figure 3). In this series, the metal center, the steric properties of the ancillary ligand and the nature of the central donor trans to hydride have been systematically varied, to establish the effects of such variations on the activity and selectivity of the CO₂ hydroboration process [48].

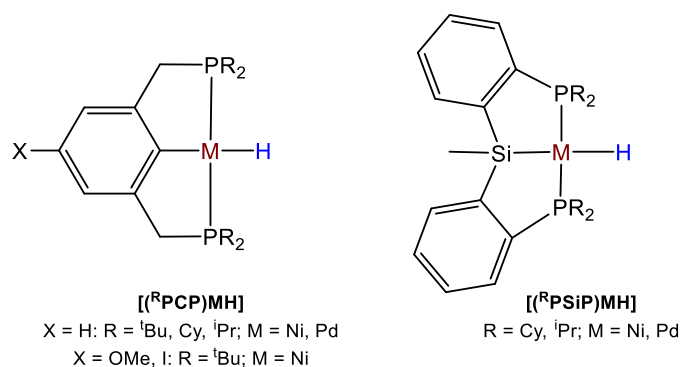
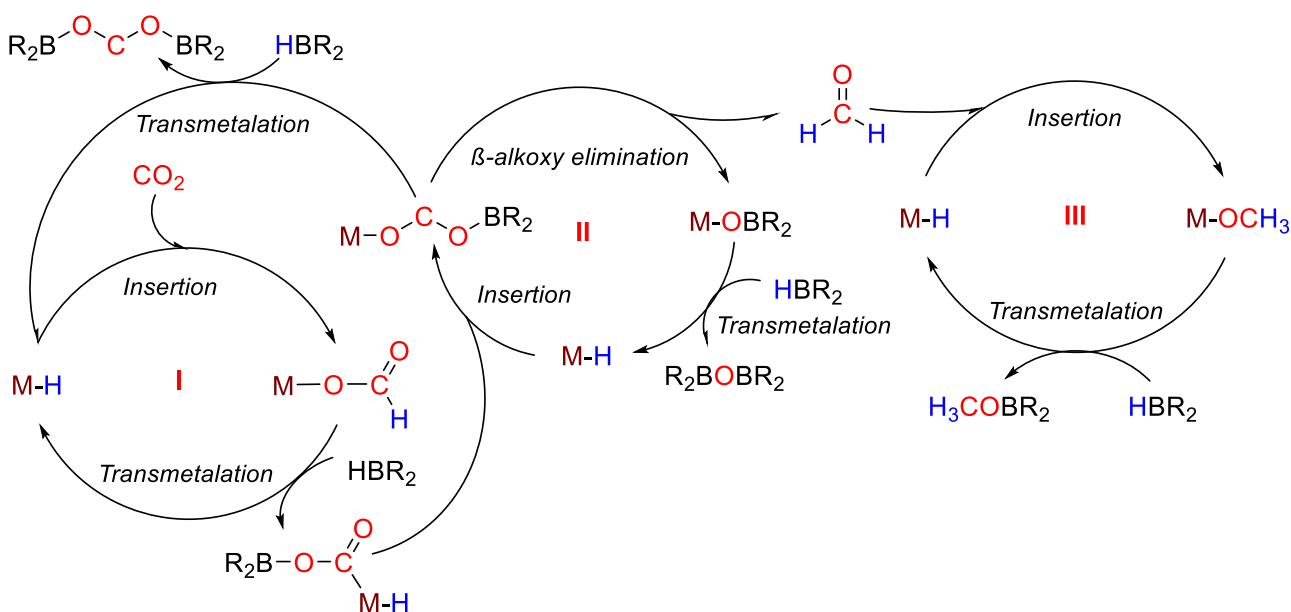


Figure 3. Drawings of complexes **20a–j** [48].

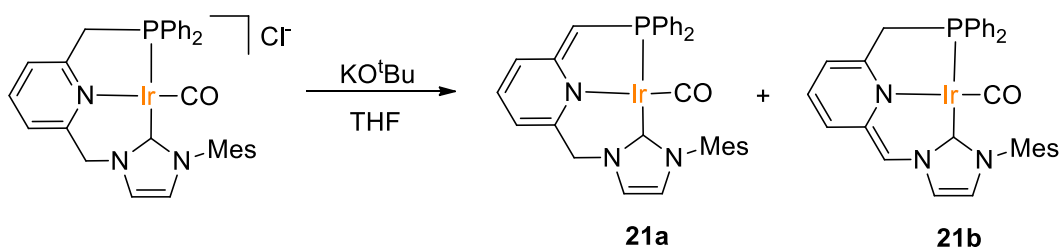
The proposed mechanism (Scheme 37) mirrors the computational studies made by Guan and coworkers for closely related systems [47]. The authors propose that CO₂ hydroboration to methoxyborane involves three sequential catalytic cycles. In the first step (cycle I), CO₂ is reduced to the formoxyborane, that is reduced to the formaldehyde in the second step (cycle II). Formaldehyde is then reduced to methoxyborane in the third step (cycle III). Each cycle requires an equivalent of borane reductant, thus the reduction to the methanol level needs 3 equiv. of borane. The relative rates of the different elementary reactions, including CO₂ vs. borane insertion, transmetalation and β-alkoxy elimination, were evaluated. The authors reasoned that preferential formation of formoxyborane may be related to a kinetic preference for CO₂ insertion over formate insertion into the M–H bond. This, in turn, implies that an equilibrium between metal formate, formed through CO₂ insertion, and metal acetal, formed through formate insertion, does not take place. The following reduction to the formaldehyde and methanol level may occur only when formate insertion becomes competitive with CO₂ insertion.



Scheme 37. Proposed mechanism for CO₂ hydroboration with **20a–j** [48].

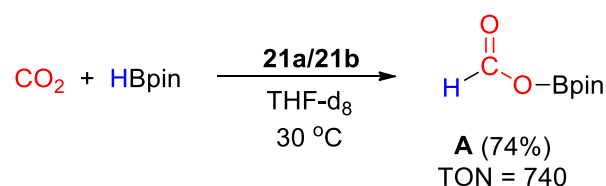
The catalytic reaction between CO₂ (1 atm) and HBpin (0.07 M) was initially tested in the presence of metal complexes **20a–j** (1 mol%) at room temperature in C₆D₆. All catalysts favored the formation of (OCHO)Bpin with yields in the range 55–89%, and the highest performance and selectivity was shown by [(^{Cy}PSiP)PdH] (**20i**). Next, the effect of CO₂ concentration was tested in the presence of [(^{tBu}PCP)PdH] (**20g**, 1 mol%). It was observed that the process selectivity changed from (OCHO)Bpin, obtained in 88% yield after one day with complete selectivity under 1 bar CO₂ (5 equivalents to borane), to a mixture of (OCHO)Bpin, (Bpin)OCH₂O(Bpin) and CH₃O(Bpin) (11, 44 and 36%, respectively), when the CO₂ pressure was reduced to 0.15 bar (0.5 equiv. to borane), albeit at longer reaction times (eight days). Then, the hydroboration of CO₂ using HBpin in the presence of [(^{tBu}PCP)PdH] (**20g**) or [(^{iPr}PSiP)NiH] (**20e**), as catalysts at varied borane concentrations, was tested. It was observed that when **20e** was used as the catalyst, significant reactivity beyond the formoxyborane product was shown at lower concentrations of HBpin than with **20g**, as ^RPSiP ligands tend to promote reactivity beyond cycle I (Scheme 37) more readily than ^RPCP ligands. Interestingly, also the ratio between products of CO₂ reduction depended on the catalyst concentration. Indeed, when the loading of **20e** was decreased from 1 to 0.1 mol %, the ratio of bis(boryl)acetal to methoxyborane increased from 1.3:1 to 2.3:1. The effect of addition of a Lewis acid co-catalyst such as B(OPh)₃ on the selectivity of CO₂ hydroboration was then studied. The addition of B(OPh)₃ (10 mol%) in all cases changed the selectivity from the formoxyborane to mixtures of bis(boryl)acetal and methoxyborane products, albeit longer reaction times were needed (1–3 days) with HBpin as reductant. High yields (up to 99%) and complete selectivities to methoxyborane were observed using HBcat (0.07 M) and **20g** (0.0007 M) under 1 bar CO₂, room temperature, 16 h and in the absence of Lewis acid additives. On the other hand, the highest yields in methoxyborane (87%) using 9-BBN were obtained in the presence of [(^{tBu}PCP)NiH] (**20b**) under the same conditions [48].

Rendón, Suarez and coworkers [49] obtained iridium(CNP) pincer-type complexes **21** as a mixture of the deprotonated “tautomeric” species, by reaction of a chloride parent complex with KO^tBu in THF (Scheme 38). The ratio between these species depends on the solvent, e.g., in the ¹H NMR spectrum registered in THF-d₈, **21a** and **21b** appear in a 9:1 ratio, whereas a **21a/21b** ratio of 4:1 was observed in C₆D₆.



Scheme 38. Synthesis of Ir(PNN) pincer complexes **21** [49].

Complexes **21a** and **21b** were used as unresolved mixture for CO₂ hydroboration under mild reaction conditions (1–2 bar CO₂, 30 °C). The reaction (Scheme 39) proceeds selectively to methoxyborane using HBcat (TOFs up to 56 h⁻¹) and to the formate level with HBpin (TOF up to 1245 h⁻¹). The addition of water had a promoting effect on the reaction rates, suggesting a role in the formation of the catalytically active species [49].



Scheme 39. CO₂ hydroboration in the presence of HBpin and complex **21a–21b** [49].

In summary, the recent contributions describing second-row transition metal catalyzed CO₂ hydroboration are focused mainly on the application of pincer-type complexes. Mechanistic details were achieved in various cases, showing, for example, that it is possible to drive the process selectivity by tuning the reaction conditions, such as solvent, temperature and use of additives, to bring about selectivity switch from two-electron to six-electron reduction of CO₂.

Finally, in Table 1 below are summarized the principal data of the catalytic reactions described above, such as solvent, temperature, time of reaction, use of additives, type of product(s) obtained and best reported TONs or TOFs for each cited original article. In Table 2 are summarized the main diagnostic NMR signals of selected complexes.

Table 1. Summary of reaction conditions, product and hydroborate types, TON or TOF (h^{-1}) for CO_2 hydroboration.

Catalyst	Metal	Amount of Cat. (mol%)	Solvent	Temp. ($^{\circ}\text{C}$)	Time	Additives	Type of Product(s) ^a (type of HBR ₂)	Best TON/TOF (h^{-1})	Ref
1a	Li	1	THF	25	10 h	-	A (HBpin)	-/10	[26]
1b	K	1	THF	25	16 h	-	A (HBpin)	-/6.25	[26]
1c	Na	1	THF	25	16 h	-	A (HBpin)	-/6.25	[26]
2	Mg	5	-	100	15 h	-	C, D (HBpin)	-/-	[27]
3	Mg	10	THF-d ₈	25	3 h	-	C, D (HBpin)	-/-	[28]
4	Si	10	C ₆ D ₆	90	10 min	-	A, D (HBpin)	-/60	[29]
4	Si	10	C ₆ D ₆	90	30 min	-	C, E ^b (BH ₃ -S(Me) ₂)	-/19.8	[29]
4	Si	10	C ₆ D ₆	90	24 h	-	C, D (HBcat)	-/0.34	[29]
5	Mn	0.072	-	100	14 h	NaO ^t Bu ^c	C, D (HBpin)	883/-	[31]
6a	Mn	1	THF-d ₈	60	24 h	B(OPh) ₃ ^d	C, D (HBpin)	-/-	[33]
6a	Mn	1	THF-d ₈	60	24 h	B(OPh) ₃ ^d	C, D (9-BBN)	-/-	[33]
7	Fe	1	CH ₃ CN	25	45 min	-	B (9-BBN)	-/-	[34]
8a	Fe	1.5	CH ₃ CN	60	24–40 h	-	B, C (9-BBN)	66/2.1	[35]
8c	Co	1.5	CH ₃ CN	60	24 h	-	B, C (9-BBN)	66/2.8	[35]
8f	Cu	1.5	THF	60	4–24 h	-	B, C (9-BBN)	59/14.8	[35]
9	Co	1	THF	50	16 h	NaHBET ₃ ^e	A, C, D (HBpin)	-/-	[36]
9	Co	1	THF	50	20 h	NaHBET ₃ ^e	E ^b (BH ₃ -S(Me) ₂)	300/15	[36]
9	Co	1	C ₆ D ₆	50	72 h	NaHBET ₃ ^e	C, D (HBcat)	-/-	[36]
10a	Ni	0.2	C ₆ D ₆	25	15 min	-	C, D (HBcat)	490/2400	[38]
10b	Ni	0.2	C ₆ D ₆	25	15 min	-	C, D (HBcat)	477/ 1908	[37]
11b	Ni	0.2	C ₆ D ₆	25	4 h	-	B (HBpin)	487/-	[39]
12a	Ni	0.5	C ₆ D ₆	25	10 min	-	C, D (HBcat)	75/7.5	[40]
12b	Ni	0.25	THF-d ₈	25	7 min	-	C, D (HBcat)	75/10.7	[40]
13g	Cu	2	THF-d ₈	50	18 h	-	A, B (9-BBN)	31/-	[41]
14	Zn	10	THF/THF-d ₈	60	16 h	-	C, D (HBpin)	-/-	[42]
15a	Zn	10	C ₆ D ₅ Br	90	20 h	-	A, B, C (HBpin)	45/-	[43]
15b	Zn	10	C ₆ D ₅ Br	60	20 h	-	C (HBcat)	16/-	[43]
16a	Zn	5	C ₆ D ₆	25	12 h	-	A (HBpin)	-/-	[44]
16a	Zn	5	C ₆ D ₆	25	4 h	-	B, C (9-BBN)	-/-	[44]
16a	Zn	5	C ₆ D ₆	25	12 h	-	C (HBcat)	-/-	[44]
17a	Ru	10	C ₆ D ₅ Br	90	45 h	-	C (HBcat)	29/-	[43]
17a	Ru	10	C ₆ D ₅ Br	90	45 h	-	A, C (HBpin)	39/-	[43]
17b	Ru	10	C ₆ D ₅ Br	100	45 h	-	A, B, C (HBpin)	60/-	[43]
18	Ru	1	CD ₂ Cl ₂	25	30 min	KOCO ₂ ^t Bu ^f	A, D (HBpin)	-/-	[46]
19	Pd	0.2	C ₆ D ₆	25	15 min	-	C, D (HBcat)	445/1780	[47]
20a–j	Pd, Ni	1	C ₆ D ₆	25	10 min–10 days	B(OPh) ₃ ^d	A, B, C (HBpin, HBcat, 9-BBN)	-/-	[48]
21a,b	Ir	0.2	THF-d ₈	30	20 min	H ₂ O ^g	A (HBpin)	740/1245	[49]
21a,b	Ir	0.2	THF-d ₈	30	20 min	H ₂ O ^g	C (HBcat)	78/56	[49]

^a Products: formoxyborane (A), bis(boryl)acetal (B), methoxyborane (C), bis(boryl)ether (D); type of hydroborane used in brackets. ^b E = [BO(OMe)]₃. Amount of additives [mol%]: ^c 0.3; ^d 10; ^e 1; ^f 2.5; ^g 1–7.

Table 2. Summary of diagnostic NMR signals for selected complexes.

Catalyst	Solvent	¹ H NMR δ (ppm)	³¹ P NMR δ (ppm)	¹¹ B NMR δ (ppm)	²⁹ Si NMR δ (ppm)	Ref.
1a	THF-d ₈	-	-	-8.2 (d, J _{BH} = 79 Hz)	-	[26]
1b	THF-d ₈	-	-	-8.0 (d, J _{BH} = 76 Hz)	-	[26]
1c	THF-d ₈	-	-	-8.2 (d, J _{BH} = 76 Hz)	-	[26]
3	DMSO-d ₆	-	-	-8.3 (d, J _{BH} = 80 Hz)	-	[28]
4	Pyridine-d ₅	9.73 (s, SiH)	-	-	-77.9 (d, ¹ J _{SiH} = 283 Hz)	[30]
5	THF-d ₈	-	48.5	-	-	[31]
6a	C ₆ D ₆	-5.72 (t, J _{HHP} = 51.4 Hz, MnH)	164.8	-	-	[32]
7	C ₆ D ₆	-14.33	83.7, 74.1	-	-	[50]
8a	CD ₃ CN	-	30.2	-	-	[35]
8b	CD ₃ CN	-	147.9	-	-	[35]
8e	CD ₂ Cl ₂	-	-33 (m, J _{PCu} ~ 840 Hz);	-	-	[35]
8f	CD ₂ Cl ₂	-	80 (m, J _{PCu} ~ 860 Hz)	-	-	[35]
10b	CDCl ₃	-	185.2	-	-	[51]
11a	C ₆ D ₆	-	36.0	-	43.8	[39]
11b	C ₆ D ₆	-4.79 (brs, NiH)	65.6	-	59.8	[39]
12a	C ₆ D ₆	-8.25 (t, J _{HHP} = 55.6 Hz, Ni-H)	205.7	-	-	[40]
12b	C ₇ D ₈	-7.90 (t, J _{HHP} = 55.2 Hz, Ni-H)	206.6	-	-	[40]
13a	CD ₂ Cl ₂	-	31.4	-	-	[41]
13b	CD ₂ Cl ₂	-	31.8	-	-	[41]
13c	CD ₂ Cl ₂	-	29.7	-	-	[41]
13d	CD ₂ Cl ₂	-	25.9	-	-	[41]
13e	CD ₂ Cl ₂	-	64.1	-	-	[41]
13f	CD ₂ Cl ₂	-	62.8	-	-	[41]
13g	CD ₂ Cl ₂	-	61.9	-	-	[41]
14	THF-d ₈	-	-	-7.9 (d, ¹ J _{BH} = 79 Hz)	-15.1	[42]
15b	C ₆ D ₆	-	-	31.40	-	[43]
16a	C ₇ D ₈	4.15 (s), 3.50 (s)	-20.0	-	-	[44]
16b	C ₇ D ₈	4.32 (s), 3.46 (s)	-19.5	-	-	[44]
17a	C ₆ D ₆	-	48.6	-	-	[43]
17b	C ₆ D ₆	-	48.5	31.30	-	[43]
18	DMSO-d ₆	-4.99 (s, Ru-H);	-	-	-	[46]

Table 2. Cont.

Catalyst	Solvent	¹ H NMR δ (ppm)	³¹ P NMR δ (ppm)	¹¹ B NMR δ (ppm)	²⁹ Si NMR δ (ppm)	Ref.
19a	C ₆ D ₆	-	189.7	-	-	[47]
19b	C ₆ D ₆	-	192.4	-	-	[47]
19c	C ₆ D ₆	-	147.8	-	-	[47]
19d	C ₆ D ₆	-	191.4	-	-	[47]
20a	C ₆ D ₆	-9.9 (t, ² JHP = 55.5 Hz, Ni-H);	66.9	-	-	[52]
20b	C ₆ D ₆	-10.0 (t, ² JHP = 52.8 Hz, NiH)	99.8	-	-	[52]
20c	C ₆ D ₆	-9.9 (t, ² JHP = 55.6 Hz, Ni-H)	78.2	-	-	[52]
20d	C ₆ D ₆	-3.50 (t, ² JHP = 46 Hz, Ni-H)	78.5	-	-	[53]
20g	C ₆ D ₆	-3.86 (t, ² JHP = 13.5 Hz, Pd-H)	-	-	-	[54]
20h	CDCl ₃	-3.77 (t, ² JHP = 17.0 Hz, Pd-H)	71.7	-	-	[55]
20i	C ₆ D ₆	1.28	81.0	-	62.5 (t, ³ J _{SiH} = 47 Hz)	[53]
20j	C ₆ D ₆	1.01 (t, ² JHP = 22.6 Hz, Pd-H)	88.3	-	60.8 (t, ³ J _{SiH} = 6.7 Hz)	[56]
21a	THF-d ₈	-	28.3	-	-	[49]
21b	THF-d ₈	-	33.3	-	-	[49]

5. Conclusions

In conclusion, in the present review article are summarized the recent contributions of research groups worldwide in the scientific literature, focusing on the synthetic aspects of metal catalyst synthesis and application to CO₂ hydroboration. Except for some articles, few mechanistic details are available, making it difficult to draw a rationale on the effects of the catalyst structure on the activity and selectivity of the process. Remarkable results have been described both with first-row and second-row transition metals, in particular Mn, Fe, Ni and Pd, setting a new state-of-the-art for the conversion of CO₂ to added value products such as HCOOH, HCHO and MeOH by hydroboration processes. The advantage of such an approach was confirmed as the possibility to use very mild conditions of temperature (in general favoring two-electron reduction), small amounts of catalysts and different hydroboranes. Under this point of view, the recent studies confirmed that the less sterically hindered HBcat favors in general six-electrons reduction to methoxyboranes. Noteworthy, recent results showed that also the challenging four-electrons reduction to bis(boryl)acetals can be achieved with high selectivity. In our view, this can be considered as one of the most likely targets for future research in the field of CO₂ hydroboration, due to the possible synthetic applications of such molecules as efficient methylene transfer reagents in organic synthesis.

Author Contributions: Writing—original draft preparation, S.K.; writing—review and editing, L.G.; supervision, L.G.; funding acquisition, L.G., M.P. All authors have read and agreed to the published version of the manuscript.

Funding: This research was funded by the Polish National Agency for Academic Exchange (grant no. PPN/BEK/2018/1/00138). This work was also supported by COST Action CA15106 CHAOS (C-H Activation in Organic Synthesis).

Institutional Review Board Statement: Not applicable.

Informed Consent Statement: Not applicable.

Data Availability Statement: Not applicable.

Conflicts of Interest: The authors declare no conflict of interest

References

1. Data from United States Environmental Protection Agency (EPA). 2018. Available online: <https://www.epa.gov/ghgemissions/overview-greenhouse-gases> (accessed on 23 November 2020).
2. Data from International Energy Agency Editions. Available online: <https://www.iea.org> (accessed on 23 November 2020).
3. Mleczko, L.; Wolf, A.; Lolli, G. New Feedstocks and Chemistry for Lower CO₂-Footprint: Today, Tomorrow, and in the Future. *ChemBioEng. Rev.* **2016**, *3*, 204–218. [CrossRef]
4. Zhang, Y.-Y.; Wu, G.-P.; Darensbourg, D.J. CO₂-Based Block Copolymers: Present and Future Designs. *Trends Chem.* **2020**, *2*, 750–763. [CrossRef]
5. Jiang, X.; Nie, X.; Guo, X.; Song, C.; Chen, J.G. Recent Advances in Carbon Dioxide Hydrogenation to Methanol via Heterogeneous Catalysis. *Chem. Rev.* **2020**, *120*, 7984–8034. [CrossRef] [PubMed]
6. Onishi, N.; Laurency, G.; Beller, M.; Himeda, Y. Recent progress for reversible homogeneous catalytic hydrogen storage in formic acid and in methanol. *Coord. Chem. Rev.* **2018**, *373*, 317–332. [CrossRef]
7. Yaashikaa, P.R.; Senthil Kumar, P.; Varjani, S.J.; Saravanan, A. A review on photochemical, biochemical and electrochemical transformation of CO₂ into value-added products. *J. CO₂ Util.* **2019**, *33*, 131–147. [CrossRef]
8. Daiyan, R.; Saputera, W.H.; Masood, H.; Leverett, J.; Lu, X.; Amal, R. A Disquisition on the Active Sites of Heterogeneous Catalysts for Electrochemical Reduction of CO₂ to Value-Added Chemicals and Fuel. *Adv. Energy Mater.* **2020**, *10*, 1902106. [CrossRef]
9. Modak, A.; Bhanja, P.; Dutta, S.; Chowdhury, B.; Bhaumik, A. Catalytic reduction of CO₂ into fuels and fine chemicals. *Green Chem.* **2020**, *22*, 4002–4033. [CrossRef]
10. Singh, A.K.; Singh, S.; Kumar, A. Hydrogen energy future with formic acid: A renewable chemical hydrogen storage system. *Catal. Sci. Technol.* **2016**, *6*, 12–40. [CrossRef]
11. Sordakis, K.; Tang, C.; Vogt, L.K.; Junge, H.; Dyson, P.J.; Beller, M.; Laurency, G. Homogeneous Catalysis for Sustainable Hydrogen Storage in Formic Acid and Alcohols. *Chem. Rev.* **2018**, *118*, 372–433. [CrossRef]
12. Zhang, Y.; Zhang, T.; Das, S. Catalytic transformation of CO₂ into C1 chemicals using hydrosilanes as a reducing agent. *Green Chem.* **2020**, *22*, 1800–1820. [CrossRef]

13. Fernández-Alvarez, L.A.; Oro, L.A. Homogeneous Catalytic Reduction of CO₂ with Silicon-Hydrides, State of the Art. *ChemmatChem* **2018**, *10*, 4783–4796. [[CrossRef](#)]
14. Fernández-Alvarez, F.J.; Aitani, A.M.; Oro, L.A. Homogeneous catalytic reduction of CO₂ with hydrosilanes. *Catal. Sci. Technol.* **2014**, *4*, 611–624. [[CrossRef](#)]
15. Tlili, A.; Blondiaux, E.; Frogneux, X.; Cantat, T. Reductive functionalization of CO₂ with amines: An entry to formamide, formamidine and methylamine derivatives. *Green Chem.* **2015**, *17*, 157–168. [[CrossRef](#)]
16. Bontemps, S. Boron-mediated activation of carbon dioxide. *Coord. Chem. Rev.* **2016**, *308*, 117–130. [[CrossRef](#)]
17. Geier, S.J.; Vogels, C.M.; Westcott, S.A. *Boron Reagents in Synthesis*; ACS Symposium Series; Coca, A., Ed.; American Chemical Society: Washington, DC, USA, 2016; Chapter 6; pp. 209–225. ISBN 139780841231832.
18. Wu, X.-F.; Beller, M. (Eds.) Chemical Transformations of Carbon Dioxide. In *Topics in Current Chemistry Collections*, 1st ed.; Springer International Publishing: New York, NY, USA, 2018.
19. Aresta, M.; Dibenedetto, A.; Angelini, A. Catalysis for the Valorization of Exhaust Carbon: From CO₂ to Chemicals, Materials, and Fuels. Technological Use of CO₂. *Chem. Rev.* **2014**, *114*, 1709–1742. [[CrossRef](#)]
20. Peters, M.; Koehler, B.; Kuckshinrichs, W.; Leitner, W.; Markewitz, P.; Mueller, T.E. Chemical Technologies for Exploiting and Recycling Carbon Dioxide into the Value Chain. *ChemSusChem* **2011**, *4*, 1216–1240. [[CrossRef](#)]
21. Aresta, M.; Dibenedetto, A. Utilisation of CO₂ as a Chemical Feedstock: Opportunities and Challenges. *Dalton Trans.* **2007**, 2975–2992. [[CrossRef](#)]
22. Pinaka, A.; Vougioukalakis, G.C. Using Sustainable Metals to Carry out “Green” Transformations: Fe- and Cu-Catalyzed CO₂ Monetization. *Coord. Chem. Rev.* **2015**, *288*, 69–97. [[CrossRef](#)]
23. Grice, K.A. Carbon dioxide reduction with homogenous early transition metal complexes: Opportunities and challenges for developing CO₂ catalysis. *Coord. Chem. Rev.* **2017**, *336*, 78–95. [[CrossRef](#)]
24. Dagorne, S.; Wehmschulte, W. Recent Developments on the Use of Group 13 Metal Complexes in Catalysis. *ChemCatChem* **2018**, *10*, 2509–2520. [[CrossRef](#)]
25. Wang, X.; Xia, C.; Wu, L. Homogeneous carbon dioxide reduction with p-block element-containing reductants. *Green Chem.* **2018**, *20*, 5415–5426. [[CrossRef](#)]
26. Mukherjee, D.; Osseili, H.; Spaniol, T.P.; Okuda, J. Alkali Metal Hydridotriphenylborates [(L)M][HBPh₃] (M = Li, Na, K): Chemoselective Catalysts for Carbonyl and CO₂ Hydroboration. *J. Am. Chem. Soc.* **2016**, *138*, 10790–10793. [[CrossRef](#)] [[PubMed](#)]
27. Cao, X.; Wang, W.; Lu, K.; Yao, W.; Xue, F.; Ma, M. Magnesium-catalyzed hydroboration of organic carbonates, carbon dioxide and esters. *Dalton Trans.* **2020**, *49*, 2776–2780. [[CrossRef](#)] [[PubMed](#)]
28. Mukherjee, D.; Shirase, S.; Spaniol, T.P.; Mashima, K.; Okuda, J. Magnesium hydridotriphenylborate [Mg(thf)₆][HBPh₃]₂: A versatile hydroboration catalyst. *Chem. Commun.* **2016**, *52*, 13155–13158. [[CrossRef](#)]
29. Leong, B.X.; Lee, J.; Li, Y.; Yang, M.-C.; Siu, C.-K.A.; Su, M.-D.; So, C.-W. A Versatile NHC-Parent Silyliumylidene Cation for Catalytic Chemo- and Regioselective Hydroboration. *J. Am. Chem. Soc.* **2019**, *141*, 17629–17636. [[CrossRef](#)]
30. Li, Y.; Chan, Y.-C.; Leong, B.-X.; Li, Y.; Richards, E.; Indu, P.; De, S.; Parameswaran, P.; So, C.-W. Trapping a Silicon(I) Radical with Carbenes: A Cationic CAAC-Silicon(I) Radical and an NHC-Parent-Silyliumylidene Cation. *Angew. Chem. Int. Ed.* **2017**, *56*, 7573–7578. [[CrossRef](#)]
31. Erken, C.; Kaithal, A.; Sen, S.; Weyhermüller, T.; Hölscher, M.; Werlé, C.; Leitner, W. Manganese-catalyzed hydroboration of carbon dioxide and other challenging carbonyl groups. *Nat. Commun.* **2018**, *9*, 4521. [[CrossRef](#)]
32. Kostera, S.; Peruzzini, M.; Kirchner, K.; Gonsalvi, L. Mild and Selective Carbon Dioxide Hydroboration to Methoxyboranes Catalyzed by Mn(I) PNP Pincer Complexes. *ChemCatChem* **2020**, *12*, 4625–4631. [[CrossRef](#)]
33. Mastalir, M.; Glatz, M.; Gorgas, N.; Stöger, B.; Pittenauer, E.; Allmaier, G.; Veiros, L.F.; Kirchner, K. Divergent Coupling of Alcohols and Amines Catalyzed by Isoelectronic Hydride Mn^I and Fe^{II} PNP Pincer Complexes. *Chem. Eur. J.* **2016**, *22*, 12316–12320. [[CrossRef](#)]
34. Desmons, S.; Zhang, D.; Fajardo, A.M.; Bontemps, S. Versatile CO₂ Transformations into Complex Products: A One-pot Two-step Strategy. *J. Vis. Exp.* **2019**, *153*, 60348.
35. Aloisi, A.; Berthet, J.-C.; Genre, C.; Thuéry, P.; Cantat, T. Complexes of the tripodal phosphine ligands PhSi(XPPh₂)₃ (X = CH₂, O): Synthesis, structure and catalytic activity in the hydroboration of CO₂. *Dalton Trans.* **2016**, *45*, 14774–14788. [[CrossRef](#)] [[PubMed](#)]
36. Tamang, S.R.; Findlater, M. Cobalt catalysed reduction of CO₂ via hydroboration. *Dalton Trans.* **2018**, *47*, 8199–8203. [[CrossRef](#)] [[PubMed](#)]
37. Zhang, J.; Chang, J.; Liu, T.; Cao, B.; Ding, Y.; Chen, X. Application of POCOP Pincer Nickel Complexes to the Catalytic Hydroboration of Carbon Dioxide. *Catalysts* **2018**, *8*, 508. [[CrossRef](#)]
38. Liu, T.; Meng, W.; Ma, Q.-Q.; Zhang, J.; Li, H.; Li, S.; Zhao, Q.; Chen, X. Hydroboration of CO₂ catalyzed by bis(phosphinite) pincer ligated nickel thiolate complexes. *Dalton Trans.* **2017**, *46*, 4504–4509. [[CrossRef](#)] [[PubMed](#)]
39. Murphy, L.J.; Hollenhorst, H.; McDonald, R.; Ferguson, M.; Lumsden, M.D.; Turculet, L. Selective Ni-Catalyzed Hydroboration of CO₂ to the Formaldehyde Level Enabled by New PSiP Ligation. *Organometallics* **2017**, *36*, 3709–3720. [[CrossRef](#)]
40. Wellala, N.P.N.; Dong, H.T.; Krause, J.A.; Guan, H. Janus POCOP Pincer Complexes of Nickel. *Organometallics* **2018**, *37*, 4031–4039. [[CrossRef](#)]
41. Smirnova, E.S.; Acuña-Parés, F.; Escudero-Adán, E.C.; Jelsch, C.; Lloret-Fillol, J. Synthesis and Reactivity of Copper(I) Complexes Based on C₃-Symmetric Tripodal HTIM(PR₂)₃ Ligands. *Eur. J. Inorg. Chem.* **2018**, 2612–2620. [[CrossRef](#)]

42. Mukherjee, D.; Wiegand, A.-K.; Spaniol, T.P.; Okuda, J. Zinc hydridotriphenylborates supported by a neutral macrocyclic polyamine. *Dalton Trans.* **2017**, *46*, 6183–6186. [[CrossRef](#)]
43. Janes, T.; Osten, K.M.; Pantaleo, A.; Yan, E.; Yang, Y.; Song, D. Insertion of CO₂ into the carbon–boron bond of a boronic ester ligand. *Chem. Commun.* **2016**, *52*, 4148–4151. [[CrossRef](#)]
44. Wang, X.; Chang, K.; Xu, X. Hydroboration of carbon dioxide enabled by molecular zinc dihydrides. *Dalton Trans.* **2020**, *49*, 7324–7327. [[CrossRef](#)]
45. Li, L.; Zhu, H.; Liu, L.; Song, D.; Lei, M. A Hydride-Shuttle Mechanism for the Catalytic Hydroboration of CO₂. *Inorg. Chem.* **2018**, *57*, 3054–3060. [[CrossRef](#)] [[PubMed](#)]
46. Ng, C.K.; Wu, J.; Hor, T.S.A.; Luo, H.-K. A binary catalyst system of a cationic Ru–CNC pincer complex with an alkali metal salt for selective hydroboration of carbon dioxide. *Chem. Commun.* **2016**, *52*, 11842–11845. [[CrossRef](#)] [[PubMed](#)]
47. Ma, Q.-Q.; Liu, T.; Li, S.; Zhang, J.; Chen, X.; Guan, H. Highly efficient reduction of carbon dioxide with a borane catalyzed by bis(phosphinite) pincer ligated palladium thiolate complexes. *Chem. Commun.* **2016**, *52*, 14262–14265. [[CrossRef](#)] [[PubMed](#)]
48. Espinosa, M.R.; Charboneau, D.J.; de Oliveira, A.G.; Hazari, N. Controlling Selectivity in the Hydroboration of Carbon Dioxide to the Formic Acid, Formaldehyde, and Methanol Oxidation Levels. *ACS Catal.* **2019**, *9*, 301–314. [[CrossRef](#)]
49. Sánchez, P.; Hernández-Juárez, M.; Rendón, N.; López-Serrano, J.; Álvarez, E.; Paneque, M.; Suárez, A. Hydroboration of carbon dioxide with catechol- and pinacolborane using an Ir–CNP* pincer complex. Water influence on the catalytic activity. *Dalton Trans.* **2018**, *47*, 16766–16776. [[CrossRef](#)]
50. Field, L.D.; Shaw, W.J.; Turner, P. Addition of Nitrogen-Containing Heteroallenes to Iron(II)-Hydrides. *Organometallics* **2001**, *20*, 3491–3499. [[CrossRef](#)]
51. Li, H.; Meng, W.; Adhikary, A.; Li, S.; Ma, N.; Zhao, Q.; Yang, Q.; Eberhardt, N.A.; Leahy, K.M.; Krause, J.A.; et al. Metathesis reactivity of bis(phosphinite) pincer ligated nickel chloride, isothiocyanate and azide complexes. *J. Organomet. Chem.* **2016**, *804*, 132–141. [[CrossRef](#)]
52. Boro, B.J.; Duesler, E.N.; Goldberg, K.I.; Kemp, R.A. Synthesis, Characterization, and Reactivity of Nickel Hydride Complexes Containing 2,6-C₆H₃(CH₂PR₂)₂ (R = *t*Bu, *c*Hex, and *i*Pr) Pincer Ligands. *Inorg. Chem.* **2009**, *48*, 5081–5087. [[CrossRef](#)]
53. Suh, H.-W.; Schmeier, T.J.; Hazari, N.; Kemp, R.A.; Takase, M.K. Experimental and Computational Studies of the Reaction of Carbon Dioxide with Pincer-Supported Nickel and Palladium Hydride. *Organometallics* **2012**, *31*, 8225–8236. [[CrossRef](#)]
54. Moulton, C.J.; Shaw, B.L. Transition Metal–Carbon Bonds. Part XLII. Complexes of Nickel, Palladium, Platinum, Rhodium and Iridium with the Tridentate Ligand 2,6-Bis[(di-*t*-butylphosphino)methyl]phenyl. *J. Chem. Soc. Dalton Trans* **1976**, 1020–1024. [[CrossRef](#)]
55. Martínez-Prieto, L.M.; Melero, C.; del Río, D.; Palma, P.; Cámpora, J.; Álvarez, E. Synthesis and Reactivity of Nickel and Palladium Fluoride Complexes with PCP Pincer Ligands. NMR-Based Assessment of Electron-Donating Properties of Fluoride and Other Monoanionic Ligands. *Organometallics* **2012**, *31*, 1425–1438. [[CrossRef](#)]
56. Suh, H.-W.; Balcells, D.; Edwards, A.J.; Guard, L.M.; Hazari, N.; Mader, E.A.; Mercado, B.Q.; Repisky, M. Understanding the Solution and Solid-State Structures of Pd and Pt PSiP Pincer-Supported Hydrides. *Inorg. Chem.* **2015**, *54*, 11411–11422. [[CrossRef](#)] [[PubMed](#)]